0254-6124/2026/46(4)-0859-32 *Chin. J. Space Sci.* 空间科学学报

GU Yidong, WANG Qiang, LÜ Congmin, LI Xuzhi, ZHONG Hongen, LIU Guoning, ZHANG Wei, ZHANG Jiuxing, BA Jin. Progress in Space Science and Utilization on the China Space Station in 2024–2026. *Chinese Journal of Space Science*, 2026, **46**(4): 859–890. CSTR:32142.14.cjss.2026–yg05. DOI:10.11728/cjss2026.04.2026–yg05

Progress in Space Science and Utilization on the China Space Station in 2024–2026*

GU Yidong WANG Qiang LÜ Congmin LI Xuzhi ZHONG Hongen
LIU Guoning ZHANG Wei ZHANG Jiuxing BA Jin

(*Key Laboratory of Space Utilization, Technology and Engineering Center for Space Utilization, Chinese Academy of Sciences, Beijing* 100094)

Abstract The China Space Station was assembled by the end of 2022, comprising three modules equipped with intravehicular science experiment racks and extravehicular exposed facilities. Operating for over three years, the station has implemented more than 170 science and utilization projects. A series of original, cutting-edge achievements has been attained in space life sciences and biotechnology, space materials science, microgravity fluid and thermal physics, microgravity combustion science, microgravity fundamental physics, and space innovative technology demonstration. This paper introduces the general progress of in-orbit science and utilization, along with typical scientific discoveries—such as the mammal on-orbit feeding experiment, growth of InSe semiconductor crystals, fabrication of high-performance field-effect transistors on ground, and observation of a metastable Body-Centered Cubic (BCC) phase in the crystallization of charged colloids. Planned science and utilization projects will be executed progressively and systematically. Furthermore, applications and transformations of these findings will be further promoted.

Key words China Space Station (CSS), Microgravity, Space science, Space utilization, On-orbit experiment

Classified index P35, V47

1 Introduction to the China Space Station

The China Space Station (CSS)[1–4] represents a comprehensive low-Earth space research platform in China. It was assembled by the end of 2022, which was in the T shape with three modules: the Core Module named Tianhe, and the Experimental Module I named Wentian, and the Experimental Module II named Mengtian. The CSS has exhibited a consistent operational stability over a period of three years, successfully accomplishing seven manned launch missions (SZ-16, 17, 18, 19, 20, 21, 23), five cargo resupply missions (TZ-6, 7, 8, 9, 10), and eight spacecraft return missions (SZ-15, 16, 17, 18, 19, 20, 21, 22), including the first emergency launch (SZ-22). Seven astronaut crew groups have participated in long-term stays in orbit, engaging in more than ten times extravehicular activities.

A suite of advanced scientific experimental racks have been deployed within the three experimental modules[4–6], including Life and Ecology experiment Rack (LER), BioTechnology experiment Rack (BTR), High-Temperature Materials experiment Rack (HTMR), Containerless Materials Processing Rack (CMPR), Fluids

* Supported by the China Manned Space Program (T3141911UN)
Received May 20, 2026

©The Author(s) 2026. This is an open access article under the CC-BY 4.0 License (https://creativecommons.org/licenses/by/4.0/)

Physics experiment Rack (FPR), Two-Phase System experiment Rack (TPSR), Combustion Science experiment Rack (CSR), High Microgravity Level Rack (HMLR), Cold Atom Physics experiment Rack (CAPR), High-Precision Time-Frequency System (HPTFS), Variable Gravity experiment Rack (VGR), Glovebox and Cold Storage Rack (GCSR), on-orbit Maintenance and Manipulation Workbench (MMW), and three extravehicular exposed experimental platform, including Exposed Radiation Biology Facility (ERBF), Exposed Materal Fcility (EMF), Exposed Component Facility (ECF). These facilities aboard the CSS have effectively supported cutting-edge scientific exploration, national needs, and technological progress. In addition, the China Space station Survey Telescope (CSST)[7] is currently under construction and it is a 2-meter caliber telescope with high-performance design. The telescope will fly and operate in conjunction with the CSS and is expected to facilitate groundbreaking researches of fundamental cosmology, such as the nature of dark energy and dark matter, galaxies and active galactic nuclei, the Milky Way and neighboring galaxies. The High Energy cosmic-Radiation Detection (HERD) facility[8] is currently under construction to support significant researches including the search for dark matter, the origin of cosmic ray, and the evolution of extreme celestial, *etc*. The expansion module is being planned to support the installation and operation of the HERD. Therefore, the basic configuration of the CSS will be upgraded from T to X. Moreover, it is worth mentioning that the space science experimental racks and extravehicular experimental facilities in various areas will further expand the science and utilization scale[9].

2 Space Science and Utilization of the CSS

Four primary research areas have been delineated: space life science and human research (including space life sciences and biotechnology, space human research), microgravity physics (including space materials science, microgravity fluid and thermal physics, microgravity combustion science, and microgravity fundamental physics), space astronomy and earth science(including space astronomy and astrophysics, space earth science, space physics and space environment), and space innovative technology and application (including space innovative technology demonstration and aerospace technology experiment).

Regular solicitation, selection, and space science and utilization projects implementations have been effectively conducted and a project research and management framework has been established. The public project solicitation and selection were conducted in 2019, 2023 and 2024, respectively. In addition, three annual summaries and evaluations (in 2023, 2024, 2025) were carried out, laying the foundation for the general progress, achievement evaluation, and project completion. The China Manned Space Agency (CMSA) has released two public "Progress Report on Scientific Research and Application of the China Space Station" (2024 and 2025)[6,10] to the society. These reports detailed a total of 67 cases of science and utilization research progress, as well as 11 cases of scientific popularization. The first academic conference concerning space science and utilization of the CSS was successfully held in Xi'an in 2024. These activities have attracted experts and scholars to actively participate in the CSS science and utilization projects.

As of 20 June 2026, the CSS had successfully deployed and implemented more than 170 science and utilization projects in orbit, achieving large number of science and utilization achievements and engineering technology breakthroughs[6,10,11]. The following section will present these achievements in detail. In the aforementioned areas of life, materials, fluid, combustion, fundamental physics, and innovative technology demonstration, a substantial body of scientific data, amounting to over 450 TB, has been obtained, and more than 500 papers have been published based on ground matching experiments, on-orbit experimental samples, and scientific data. The space materials science and technology special issue has been published in *SCIENCE CHINA Technological Sciences*, and the scientific data simulation special issue of the CSST has been published in *Research in Astronomy and Astrophysics*. These achievements and breakthroughs have had a significant impact on the development of space science and utilization in China. A preliminary investigation has been made regarding applications and transformations.

3 Space Life Science and Biotechnology

The area of space life science and biotechnology focuses primarily on fundamental biology, space life ecology, space biotechnology and its applications, as well as the origin of life and interdisciplinary research in space. A multi-level research system has been established that spans from the molecular and cellular levels to tissues, organs and individual organisms. The system elucidates the mechanisms and response patterns through which the space environment impacts life at various levels. Thirty-nine projects (statistics as of 20 June 2026) have been successfully implemented in orbit, achieving significant advancements in cell biology, botany, zoology, protein crystallization, the origin of life and radiation biology aboard the CSS. The progress and achievements have sparked new ideas and strategies, also yielding novel concepts and methodologies for the prevention and treatment of associated pathologies, the design and formulation of related pharmaceuticals, the cultivation of space plants, and the building of experimental platforms, among other applications.

3.1 The First Mouse Experiment aboard the CSS

The primary technology verification had been conducted for mouse feeding based aboard the CSS, thereby overcoming the efficient and precise biological control technology for mammals in small enclosed spaces[10,12]. The first small mammal feeding device for the CSS was independently developed, and a comprehensive process experimental system for small mammals was established in China. Four SPF grade C57 BL/6 JNifdc experimental mice that had been screened and trained were sent to the CSS, where they completed a 14-day space-enclosed mice feeding experiment in orbit[10] (Figure 1). During the on-orbit period, the intelligent observation system was utilized to record the real-time movement trajectory, feeding frequency, and sleep patterns of mice. It was found that mice adapted to the microgravity environment of the CSS, exhibiting normal behavioral rhythms and stable states. After completing the on-orbit experiment, the mice were successfully returned with the Shenzhou 20 crew. On the ground, the mice successfully were pregnant and gave birth to offspring. This preliminary finding indicated the safety of short-term spaceflight on the constructed mammalian reproductive system, and some behavioral differences were observed.

This experiment is the first to implement on-orbit feeding and scientific experiments aboard the CSS, expanding the categories and contents of space life science experiments in China. It provides important first-hand data for the study of microgravity effects and behavioral research of various organs in space mice, the exploration opportunity of the research paradigm of small sample sharing and multidimensional big data analysis of space mammals, and the preliminary research on key indicators of mouse behavior, physiology, and biochemistry. In the future, the research team will further explore the response of mouse multi-organ systems to the space



Fig. 1 In-orbit experiment photo of mice[10]. (a) Daytime working lighting, (b) night infrared lighting

environment, as well as changes in behavior, growth and development, reproductive behavior, and aging processes throughout the entire life cycle, and explore relevant mechanisms to deeply reveal the biological effects of microgravity, radiation, and other factors. The experiment lays an important foundation for the development and construction of the space mammal experimental platform to support systematic research on mammalian space science for the future.

3.2 A *Drosophila* Study: Biological Effects of Two Space Factors, Microgravity and Hypomagnetic Field

During evolution, terrestrial organisms have adapted to Earth's physical environment, particularly to Earth's Gravity (EG) and the Geomagnetic Field (GMF). In outer space, however, both parameters are drastically reduced, typically to less than 1‰ of their terrestrial levels. Even on nearby planetary bodies such as the Moon and Mars, the gravitational acceleration is only about 1/6 and 1/3 of that on Earth, respectively. Moreover, compared to the GMF, which ranges from 25 to 65 μT, the magnetic fields on the Moon (<300 nT[13,14]) and Mars (approximately 300 nT to 5 μT[15]) are substantially weaker, representing a HypoMagnetic Field (HMF) environment. Consequently, during deep-space exploration missions, Earth-originated organisms, including humans, will inevitably be exposed to these extreme physical conditions.

To investigate the biological effects of these two environmental factors, we developed *Drosophila* Research Module equipped with both GMF and HMF units aboard the CSS, operating under MicroGravity (MG) conditions. An identical module was employed as a ground-based control (Figure 2a, b). For both situations, temperature and humidity were maintained at (25 ± 1)℃ and (50% ± 5%) RH, respectively. During the 40-day experimental period, the Magnetic Field intensity (MFint) was monitored in all four units. The MFint in the on-orbit GMF unit was (4.99 ± 0.15) $\times 10^4$ nT, which was comparable to that in the ground-based GMF unit in Beijing, (4.81 ± 0.00) $\times 10^4$ nT. In contrast, the MFint in the HMF units was significantly lower, measuring (1.31 ± 0.01) $\times 10^2$ nT in the ground unit and (1.12 ± 0.02) $\times 10^2$ nT in the on-orbit unit. Accordingly, the experi-

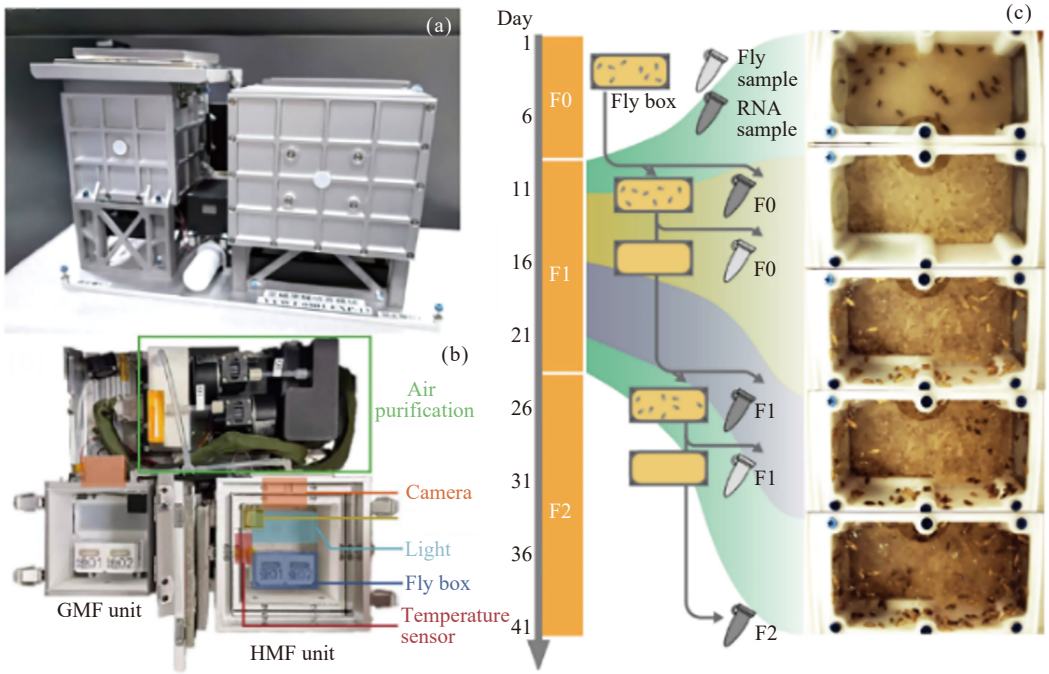


Fig. 2 *Drosophila* research module and procedures for multi-generational cultivation under combined microgravity and hypomagnetic conditions. (a) External appearance of the custom-designed module used aboard the CSS. (b) Internal configuration of the module, showing the GMF and HMF units. (c) Schematic timeline of the three-generation cultivation, concurrent on-orbit and ground-based sampling, and video acquisition

ment was conducted in four parallel groups, EG+GMF, EG+HMF, MG+GMF, and MG+HMF.

Utilizing these two parallel modules, we successfully conducted consecutive *Drosophila* cultivation for three generations both aboard the CSS and on the ground. As illustrated in Figure 2(c), the entire developmental process and adult behaviors were continuously monitored *via* video recording. Concurrently, fly samples from each generation were collected on the same schedule in orbit and on Earth. Through integrative analyses of the video data and transcriptomic profiles from the collected samples, this study enables a systematic investigation into the biological effects of gravity, magnetic fields, and their interaction across developmental, behavioral, and gene expression levels. To our knowledge, this represents the first biological investigation under two space environments, MG and HMF. The findings are anticipated to illuminate the potential challenges that Earth organisms may encounter during deep space exploration, and to guide the formulation of adaptive strategies for future interplanetary missions.

The SpaceAnimal Dataset[16] was constructed to support behavior analysis in complex spaceflight scenarios, covering three representative model organisms, including *Drosophila, Caenorhabditis elegans*, and zebra fish. Based on this dataset, a structure-aware pose estimation algorithm and a dual-stream fusion-based multi-object tracking framework were further developed, enabling high-precision pose estimation and trajectory tracking for space animal behavior analysis[16–18].

3.3 Seed-to-Seed Growth of Rice under Microgravity

The responses of plants to space environmental factors can affect adaptation and genetic stability of important agronomic traits of crop. However, the mechanisms priming crop plant response to space environment for the completion of the seed-to-seed have not been elucidated. We have finished the experiments of *Arabidopsis thaliana* from seed-to-seed on board the Chinese space lab TG-2 and the CSS, which found potential regulatory modules to integrate microgravity signals into flowering pathways in plants grown in space (Figure 3)[19–21]. The completion of the CSS provides us with a new permanent space experimental platform for long-term plant research in space. The rice had completed life cycle from seed-to-seed under microgravity aboard the CSS (Figure 4)[22]. As we know, this is the first space experiment achieving the complete rice life cycle from seed to seed in space.

Some of these space rice seeds have been used to subsequent experiments to successfully produce a fourth generation after returning to the Earth. Analyses of the mature space seeds and samples collected by astronauts in orbit indicate that rice has an excellent space adaptation ability, but some negative characteristics have also been found, such as altered phenotypes[19–21,23], small seeds, decreased seed setting rate and altered starch particle morphology. The rice phenotypic changes under

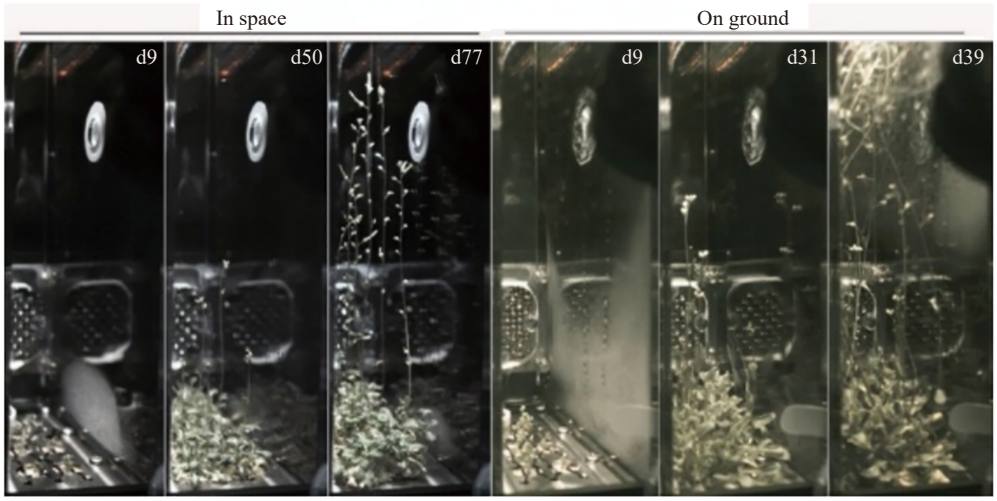


Fig. 3 Time-course series of digital images showing the growth and development of *Arabidopsis* plants grown in space and on ground



Fig. 4 Time-course series of digital images showing the growth and development of rice plants grown aboard the CSS.
(a) Time-course series of digital images showing the growth and development of rice plants grown in space,
(b) diagram showing transition time of developmental stages of rice in space,
(c) enlarged spike images of rice plants grown in space

microgravity conditions were observed, including abnormal increases in leaf angles, high-position tillering, unclosed glume, and unique stomatal structures in leaves, along with transcriptomic data.

Subsequent plants were grown from space developed parental seeds in field on Earth with higher germination rate, demonstrating the viability and reproductive capacity of rice seeds developed in the CSS, indicating the possibility of cultivating the important food crop rice throughout its entire life cycle under the spaceflight environment. However, we are now going beyond plant survival in space, but to develop a biological life support system with higher resource-use efficiency, which needs higher-yield plants. Thus, we suggest that a systematic analysis of genetic stability within consecutive multi-generation for rice plant should be performed to understand the mechanism of plant adaptation to long-term spaceflight conditions. In addition, key genes with significant application value should be identified for developing new germplasm resources with high yield, which is required for establishing reliable and efficient BLSS.

3.4 Microgravity Induces Lipid Droplet Accumulation in Hepatocytes

Although spaceflight is well documented to disrupt hepatic lipid homeostasis, the molecular mechanisms underlying gravitational sensing and mechanotransduction in hepatocytes remain incompletely elucidated. To bridge this gap, a team from the Institute of Mechanics, CAS (Chinese Academy of Sciences) has conducted an integrated *in vitro* study aboard the CSS, examining hepatic Huh-7 cell line cultured under both static and shear-flow conditions during real microgravity exposure[24]. Their findings demonstrate that microgravity induces pathological intracellular lipid droplet accumulation in Huh-7 cells under static culture, whereas physiologically relevant shear flow significantly attenuates this phenotype. Transcriptomic and proteomic analyses identify Sterol Regulatory Element-Binding Proteins (SREBPs) as central mediators: microgravity activates SREBPs, thereby upregulating *de novo* lipogenesis and cholesterol biosynthesis. Mechanistically, microgravity-triggered disassembly of F-actin cytoskeleton is shown to be sufficient for SREBP activation. Conversely, shear flow preserves F-actin architecture and suppresses SREBP nuclear translocation. Collectively, these results identify SREBPs as gravity-sensitive regulators of lipid accumulation in hepatocytes, highlighting potential therapeutic targets for maintaining liver health in space travelers during long-duration missions (see Figure 5).

3.5 Effects of Microgravity on Skeletal Muscle Cell Autophagy and miRNA Regulation

During spaceflight, adaptive atrophy of skeletal muscle poses a serious threat to astronaut health and mission performance. A team from the Shanghai Institute of Nutrition and Health, CAS, focuses on the biological basis of the effects of space microgravity on skeletal muscle. They utilized a biotechnology experimental cabinet to successfully achieve on-orbit culture and differentiation of mouse skeletal muscle cells. A skeletal muscle cell-based autophagy fluorescence reporter system was employed, in combination with space-ground comparative analysis and high-throughput sequencing, to obtain the gene expression profile of skeletal muscle cells in space. The study identified that dysregulated molecule during spaceflight can influence skeletal muscle autophagy during exercise by modulating lactate levels[25] (Figure 6). Furthermore, based on miRNA sequencing data from recovered cells and their culture media, the patterns of alterations in miRNA expression and secretion in skeletal muscle cells under space culture conditions were revealed[26]. Subsequently, the regulatory mechanism by

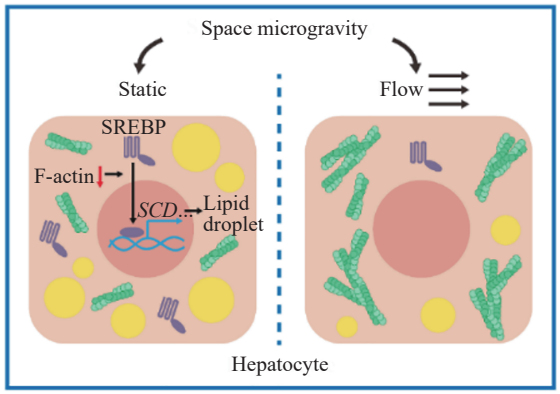


Fig. 5 Shear flow alleviates spaceflight-induced hepatic lipid dysregulation[10]

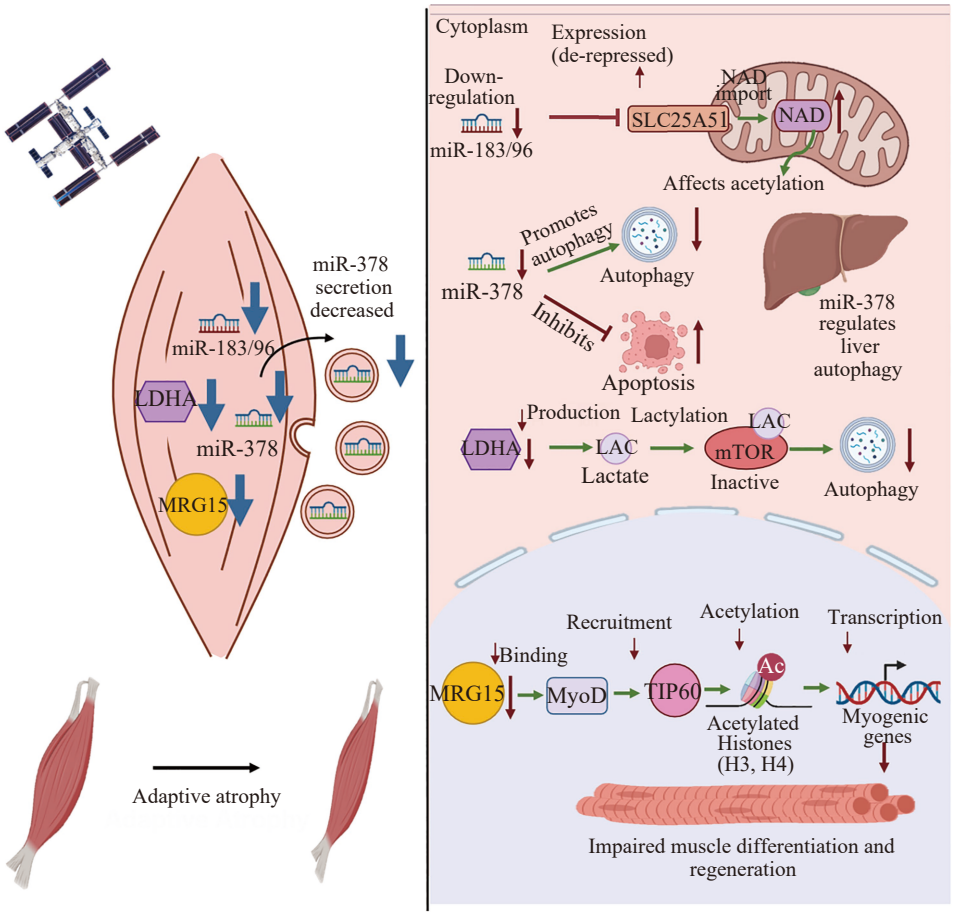


Fig. 6 Summary model diagram of the mechanism of action of dysregulated molecules in skeletal muscle cells during space flight

which dysregulated miRNAs (in terms of expression and secretion) in space culture mediate skeletal muscle stem cell dysfunction and systemic metabolic abnormalities was elucidated[27,28]. In addition, this study uncovered the regulatory mechanism of aberrantly expressed chromatin regulator in the space environment on skeletal muscle stem cells and skeletal muscle regeneration[29]. These findings provide new strategies for the prevention and treatment of muscle atrophy-related diseases.

3.6 Protein Crystallization Experiment from Space Microgravity Conditions

The changes in the interaction between water and protein molecules caused by microgravity environment in the solution can improve crystal performance and enhance resolution. With the construction of the CSS, special conditions were provided for the biotechnology development, such as protein assembly. In addition, the experimental facilities were designed and arranged for the assembly and application of the protein drug molecules, and for the preparation of single crystals of medicinal proteins/nucleic acids and their small molecule complexes in this platform.

Various proteins had been screening under high-throughput crystallization conditions for 180 days in the microgravity environment. The results show that four types of protein single crystals were obtained, which were absent under normal gravity conditions. In addition, 11 types of protein crystals have better resolution.

We also performed protein crystallization screening on the T6 topoisomerase II ATPase domain. High-quality protein crystal samples were obtained (Figure 7a), and a local view of the active center was different from cryo-EM (Figure 7b), clearly indicating the binding sites of ATP (Figure 7c), and the good electron cloud density clearly demonstrated the differences between the two catalytic centers. One subunit is a binding site for Mg^{2+}, while the other subunit is completely different. A new magnesium binding mode in ATPase type II topoisomerase of T-even bacteriophage had been revealed [10,30]. These results are important for understanding its catalytic mechanism and dynamic process, and provide important structural parameters and new ideas for future related drug design.

3.7 Abiotic Synthesis of Peptides and Nucleotides

Exploring the origin of life in space and searching for

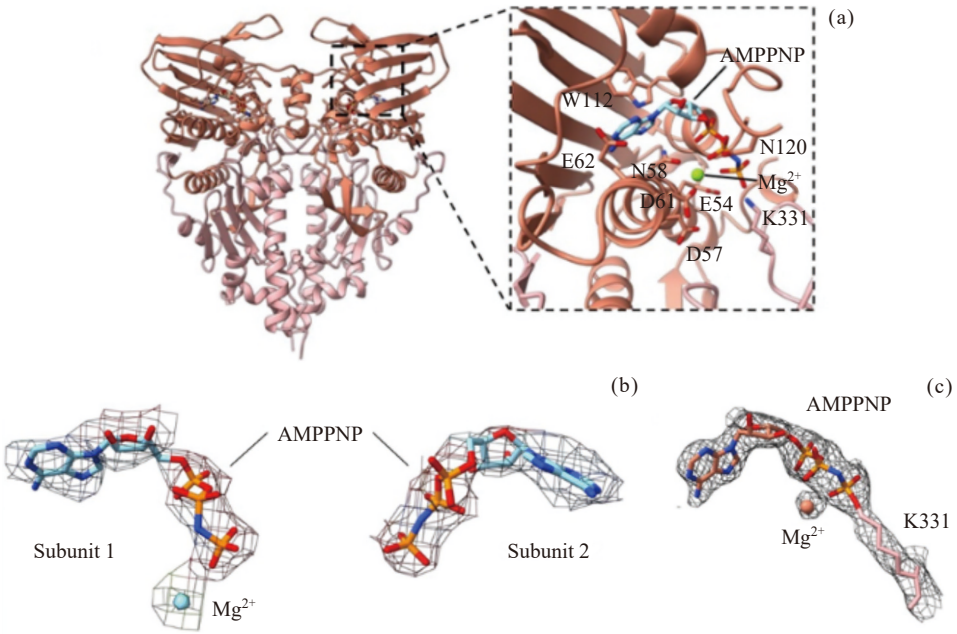


Fig. 7 Protein samples returned from on-orbit test[10,30]. (a) Overall structure of the T6 Topo II ATPase domain crystal and a local view of the active center. (b) The local density of magnesium ions and AMPPNP in the two active centers of the cryo-EM. (c) The local density of magnesium ions and AMPPNP in the active center of the crystal structure

extraterrestrial life are of great significance for the development of space resources and the expansion of human habitats. From the Murchison meteorite to the asteroids Ryugu and Bennu, the relevant findings have demonstrated that amino acids, nucleobases, ribose, and other life-related organic molecules are extensively distributed in the universe. By utilizing the extravehicular exposure platform for radiation biology of the CSS, a research team from Xiamen University investigated the feasibility of solid-phase condensation reactions of these "prebiotic organic molecules" driven by the coupling effect of ionizing radiation and forsterite. The cumulative effect of long-term, low-dose ionizing radiation under the coupling effect with forsterite was found to not only drive the formation of various dipeptides and the phosphorylation of nucleosides but also facilitate the formation of aminoacyl-adenylate analogues. Forsterite plays important auxiliary roles in this photochemical reaction process by providing an alkaline environment, electrostatic adsorption, interface catalysis centered on magnesium ions, and radiation resistance. The experiments were performed outside the Mengtian Module of the CSS. Both the sample containers and the integrated experimental units were fabricated from polyimide, which can effectively shield against UV radiation and expose the reaction systems to space ionizing radiation[31].

In addition, an investigation was conducted to focus on the influence of microgravity on prebiotic chemical reactions by utilizing a ternary chemical model that includes phosphorus activation, peptide formation, and phosphorylation of nucleosides in the Wentian Module of the CSS. The entire experimental system is placed in an SPU (Standard Payload Unit) drawer (Figure 8). It is equipped with a centrifuge for online sample mixing (Figure 8a) and four fan-shaped microfluidic chip experiment units (Figure 8b–d). The reaction process is monitored through miniature electrochemical sensors (Figure 8e).

3.8 Research on Technologies for Mining Space Radiation Biological Markers from High-Dimensional Data on Small Samples

Space radiation is one of the most significant health risks in manned space missions. Molecular markers of space radiation and techniques for assessing radiation doses are considered key bottlenecks affecting the accuracy of radiation monitoring, damage assessment, and health risk warning. In response to the environmental factors present in space biology data and the multi-omics characteristics of different dimensions such as "small samples, high dimensions", the research team led by Professor Sun Yeqing from the Institute of Environmental Systems Biology at Dalian Maritime University has developed a series of technologies integrating feature selection, cross-species comparison, and single-sample network analysis to explore the mechanisms of space radiation damage and sensitive molecular markers. By deeply coupling genetic algorithms with multiple ma-

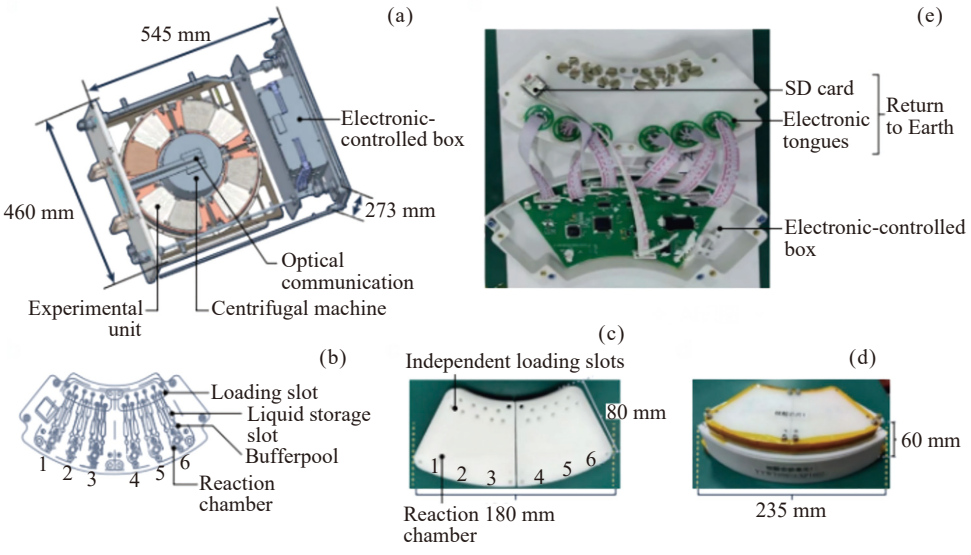


Fig. 8 Schematic view of origin of life space experiment[32]

chine learning models, the study identified key genes responsive to space radiation and established a method applicable for radiation dose assessment. Multi-omics data from different model organisms of different batches (with different exposure doses) were analyzed and verified.

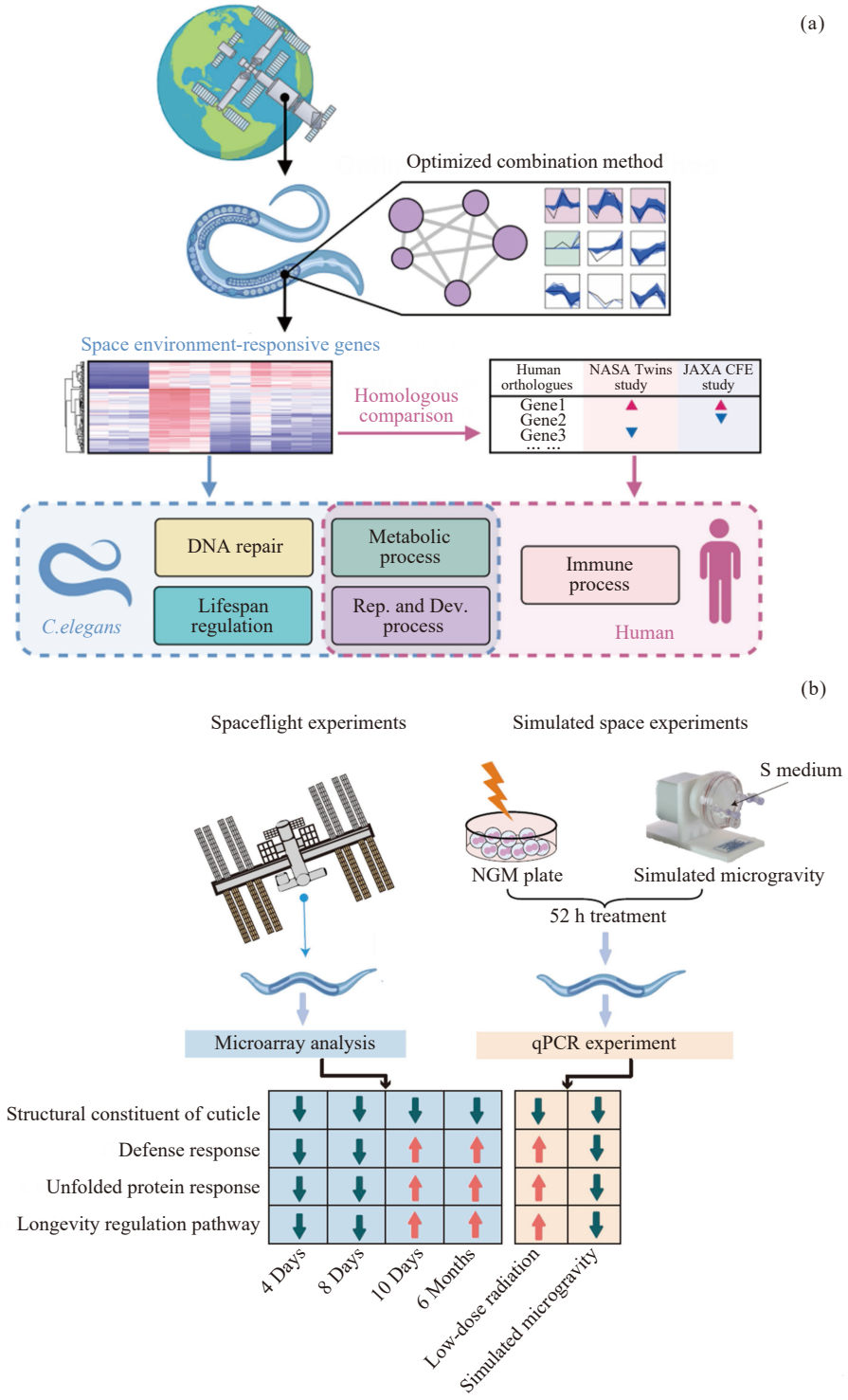


Fig. 9 Integrated spaceflight multi-omics profiling identifies novel spaceflight-responsive genes and their biological functions in *C. elegans*. (a) Comparison with astronaut peripheral blood transcriptomic data[10,33]. (b) Validation using ground-based low-dose ionizing radiation and simulated microgravity datasets[10,34]

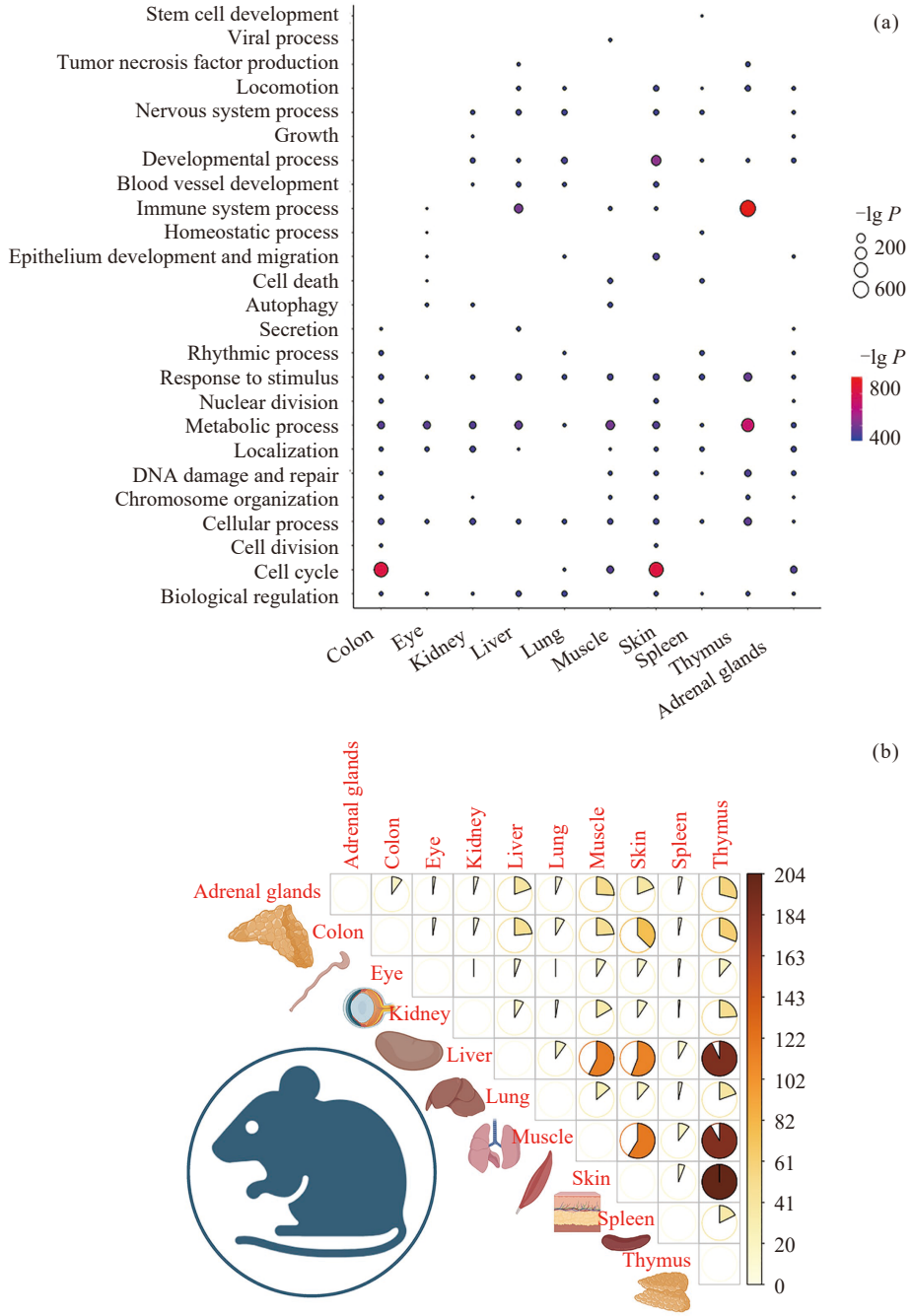


Fig. 10 Differentially Interacting Genes (DIGs) and their functions in different tissues of mouse under the space environment[10,35]. (a) The intersection of DIGs in ten tissues. The size and color of the fans represent the number of overlapping DIGs in the two tissues. (b) GO enrichment result for DIGs in ten tissues

The results show that the conservation molecular response mechanisms of invertebrates and humans to the space environment have been revealed (Figure 9a)[10,33]. The discovery of the cumulative effect of space radiation leads to a stronger molecular stress response and adaptive regulatory characteristics (Figure 9b)[10,34]. The key molecules sensitive to space radiation and their functional characteristics have been identified, the types of sensitivity and disease risks in different tissues and organs have been obtained, and a dose prediction model based on space radiation sensitivity genes has been constructed to conduct a systematic analysis and prediction of health risks induced by the space environment[10,35–37] (Figure 10–12).

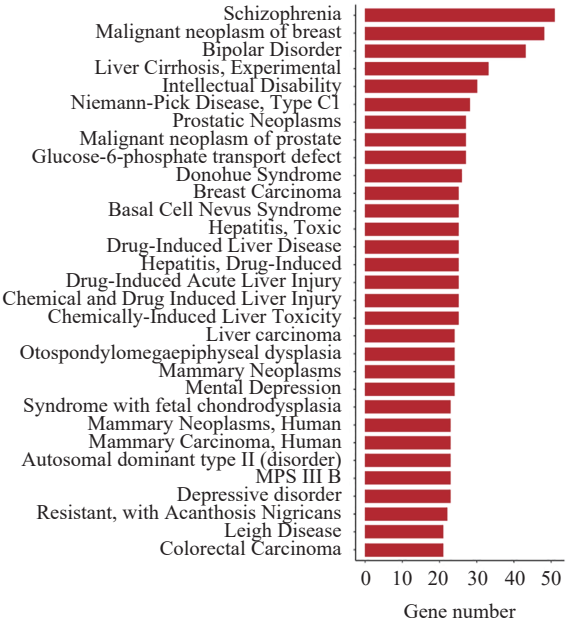


Fig. 11 Disease risk prediction using the human homologous genes of differentially interacting genes (DIGs) identified in space-flown mouse[10,35]

4 Space Materials Science

The area of space materials science focuses primarily on the mechanisms and processes involved in the preparation of materials under microgravity, novel materials and fabrication technology for important applications, service behavior of space application materials, *etc*. Seventy four projects (statistics as of 20 June 2026) have been successfully implemented in orbit. A series of significant studies and experiments were conducted in space environments, encompassing the structures, properties and physicochemical processes of various materials, the solidification mechanism of space high-temperature alloys, the macroscopic performance control mechanisms, and the operational behavior in space. Significant discoveries and breakthroughs have been made in the solidification of refractory alloys and performance regulation, semiconductor crystal growth and fabrication, microstructures and thermophysical properties measurements, lubricant materials service behavior in space, *etc*. The progress and achievements have enriched and developed the fundamental theory of research in related materials science, with some preliminary applications being attempted.

4.1 Growth Characteristics of Refractory Alloys

In containerless solidification experiments aboard the CSS, (Nb) dendrites in hypoeutectic and eutectic Nb-Si alloys preferentially form at the junctions of eutectic cells. At low undercoolings, they exhibit two-dimensional symmetric growth, at high undercoolings, three-dimensional oriented growth dominates, and dendrite tips deviate from the classical parabolic shape into dome-like, finger-like, and needle-like non-parabolic morphologies[38]. Independent Nb_3Si dendrites (decoupled growth) are observed in hypoeutectic and eutectic alloys. In the hypereutectic Nb-Si-Zr alloy, the primary phase changes from equilibrium Nb_5Si_3 to metastable Nb_3Si at large undercoolings, forming columnar or flaky dendrites[39]. In the hypoeutectic Nb-Si alloy, low undercooling produces a mixture of lamellar and rod-like eutectic; high undercooling induces a sequential transition from worm-like to lamellar and faceted eutectic[38] (Figure 13). In the eutectic Nb-Si alloy, low undercooling yields radial lamellar eutectic; at high undercooling,

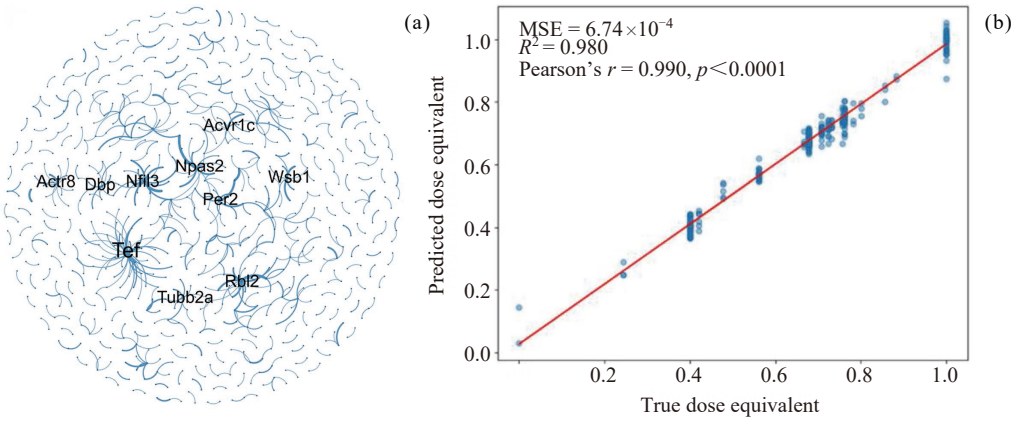


Fig. 12 Mining of key response genes (a) and space radiation dose prediction (b) in mice under space environment[10,35]

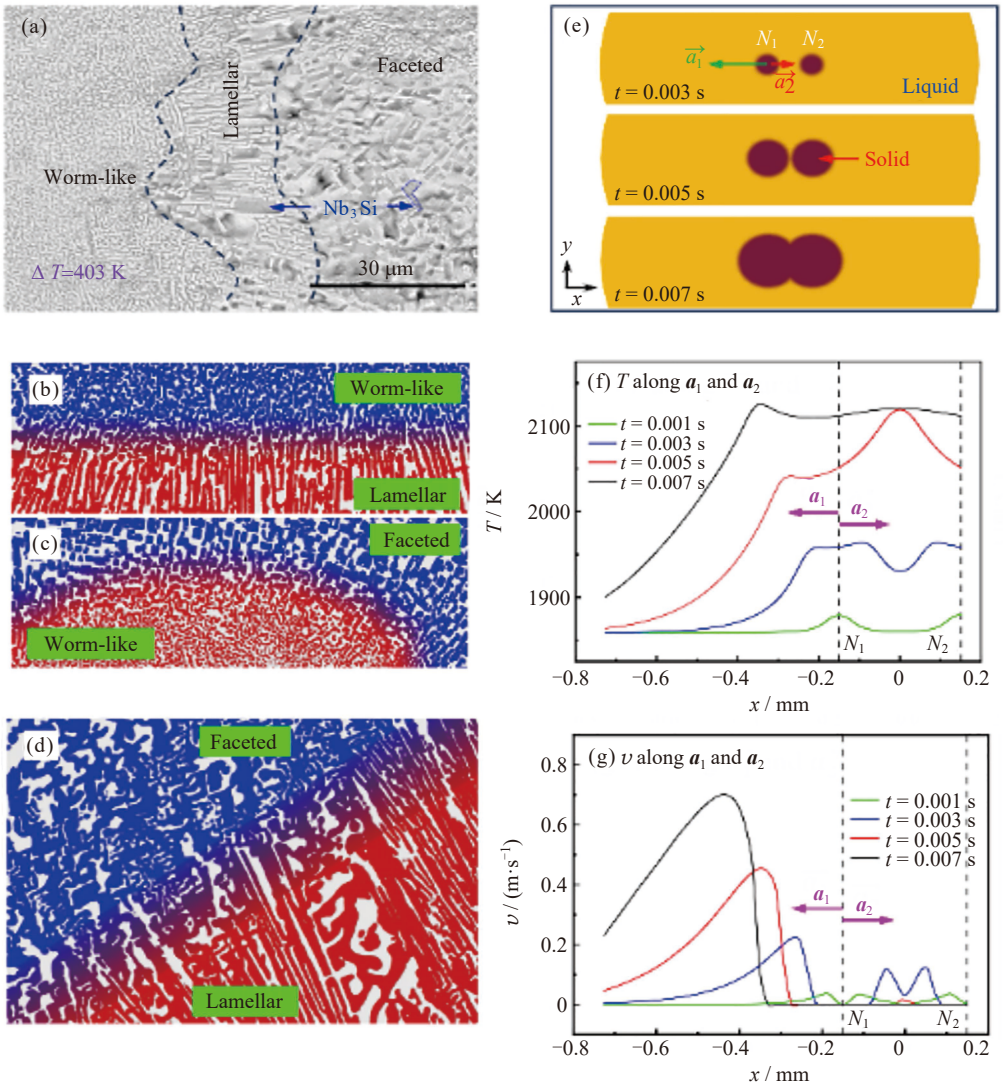


Fig. 13 Various eutectic growth modes solidified at large undercoolings under microgravity and the numerical simulation[10,38]

worm-like eutectic appears near nucleation sites and rod-like/short-lamellar eutectic at cell boundaries. In the hypereutectic Nb-Si-Zr alloy, irregular faceted, irregular lamellar-like, and regular lamellar eutectics are observed[39]. Under microgravity, the eutectic and dendritic zones exhibit spatially ordered separation, whereas buoyancy-driven convection on the ground disrupts this order.

This work systematically reveals the multi-mode transition of eutectic structures in refractory alloys under space microgravity, establishing a synergistic control mechanism of temperature gradient and absolute temperature on eutectic morphology.

A distinctive ripple-like microstructure composed of anomalous eutectic was observed in the $Zr_{57}V_{43}$ alloy solidified under microgravity. Driven by the combined effects of internal microflow and compositional fluctuations, the (Zr) and V_2Zr phases are arranged alternately like water ripples along the direction of heat flow, ultimately forming a distinctive ripple-like microstructure. The ripple-like structure also contributes to improved mechanical properties. The anomalous eutectic and finer lamellar eutectic lead to increases of 11.7% and 13.2%, respectively, in the micro-indentation hardness of the $Zr_{57}V_{43}$ alloy compared with that of the alloy solidified on the ground at a similar undercooling[40].

4.2 Ultra-High Temperature Materials Science Experiment

The CMPR had operated stably for over five years[41]. The breakthroughs had been made and multiple indepen-

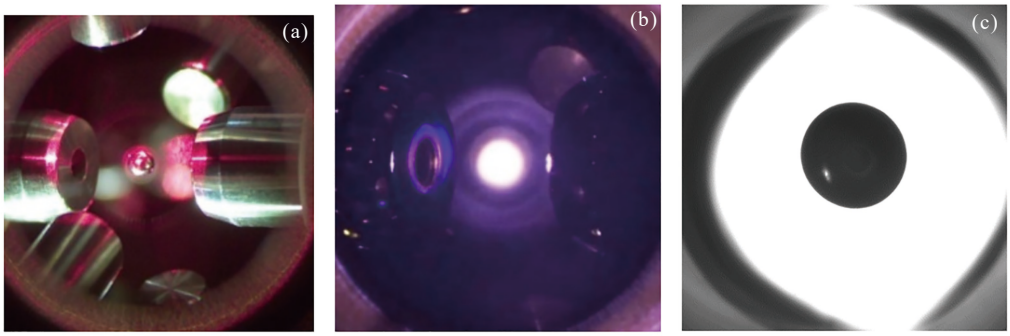


Fig. 14 Sample experimental process. (a) Stable suspension in space, (b) heating and melting of samples, (c) measurement of melt density

dently controllable key technologies had been mastered, including long-term stable electrostatic levitation under microgravity, multi-beam laser composite heating, single/dual-wavelength coupled ultra-high-temperature infrared thermometry, and high-precision thermal property measurement. The full experimental process had been standardized for the containerless materials science experiments in space (Figure 14), a high-fidelity containerless scientific matching experimental platform and digital twin model had been established, and the novel experimental mode of "space-ground collaboration + digital experimentation" had been implemented[42]. We have successfully achieved laser heating and thermal property measurement of materials at 3100℃ under microgravity, obtaining space-based solidification characteristics and critical thermal property data of ultra-high-temperature melts.

The CMPR has become a crucial space laboratory for studying the behavior of refractory metal melts. Space-based ultra-high-temperature materials science experimental techniques can support the researches on the solidification mechanisms of refractory metals and on deep undercooling and non-equilibrium solidification, the design of new high-temperature materials, and the database of thermophysical property. These techniques can enable the acquisition of intrinsic thermophysical property data of melts that cannot be obtained on ground, laying a solid experimental foundation for the design and development of ultra-high-temperature materials in China.

4.3 InSe Semiconductor Crystal Growth

Microgravity in space provides a unique environment for the growth of high-quality semiconductor crystals, especially for layered materials that are highly sensitive to convection, sedimentation, and compositional segregation during solidification. Researchers from Shanghai Dianji University and Shandong University achieved the microgravity growth of InSe aboard the CSS and subsequently fabricated high-performance Field-Effect Transistors (FETs)[43]. Spherical Aberration Corrected Scanning Transmission Electron Microscope (AC-STEM) demonstrates that the as-grown space InSe exhibits expanded atomic microstructure and lattice constants compared with the InSe grown on the ground. The as-grown space InSe possesses a γ phase similar to the ground-grown InSe, but with significantly reduced intrinsic defects. The natural space environment eliminates the sedimentation/flotation and convection driven by the effect of gravity and facilitates high-quality single crystal growth. In addition, the larger defect formation energy induced by lattice expansion contributes to the improvement of crystal quality, thus boosting the electrical and photoelectrical performance of the FETs (Figure 15).

Meanwhile, a collaborative report from Shanghai Dianji University and East China Normal University shows that the unique microgravity environment can effectively annihilate the naturally existing stacking faults in flexible InSe, thereby directly activating its intrinsic sliding ferroelectricity with excellent retention stability[44]. The corresponding ferroelectric semiconductor field-effect transistors present obviously large non-volatile memory window, high on/off ratio, and excellent mobility (Figure 16). More importantly, they also show superior amplified spontaneous emission with exceptionally low excitation thresholds of photons, indicating strong potential for near infrared nonlinear light sources. These findings not only present an unconventional strategy for achieving high-quality Van der Waals

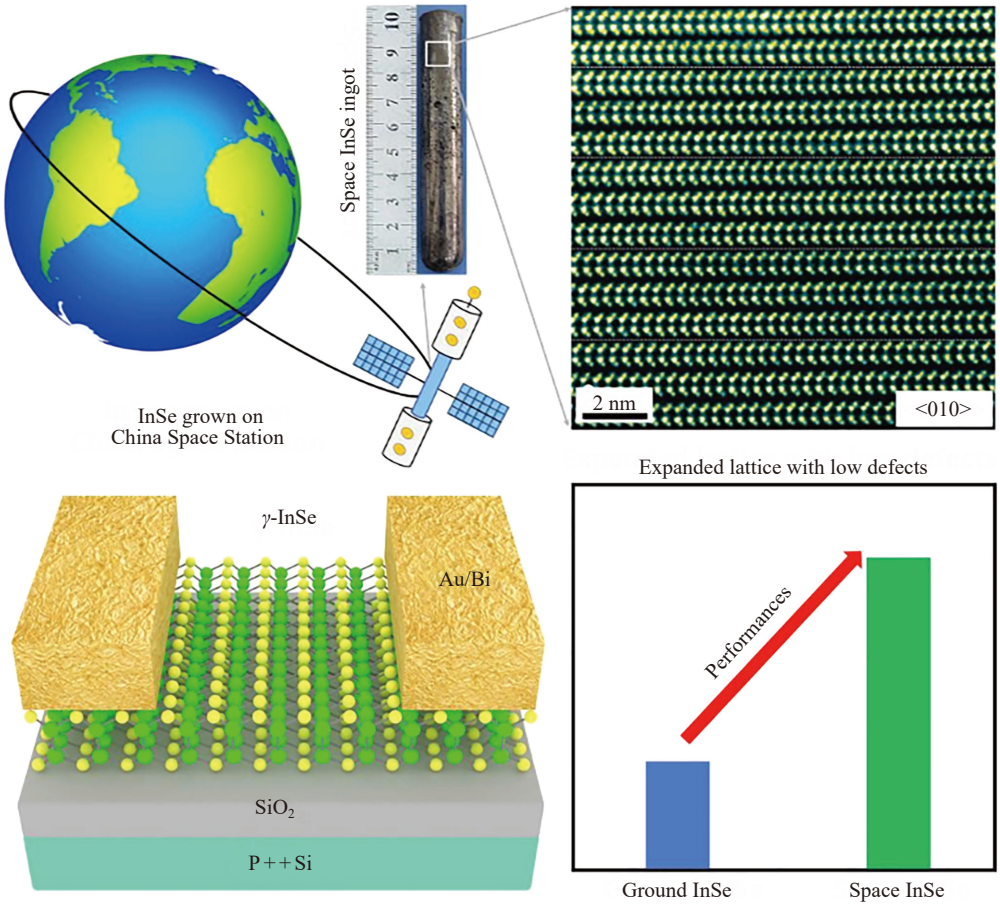


Fig. 15 Microstructure of space grown InSe crystal and high performance field-effect transistors[43]

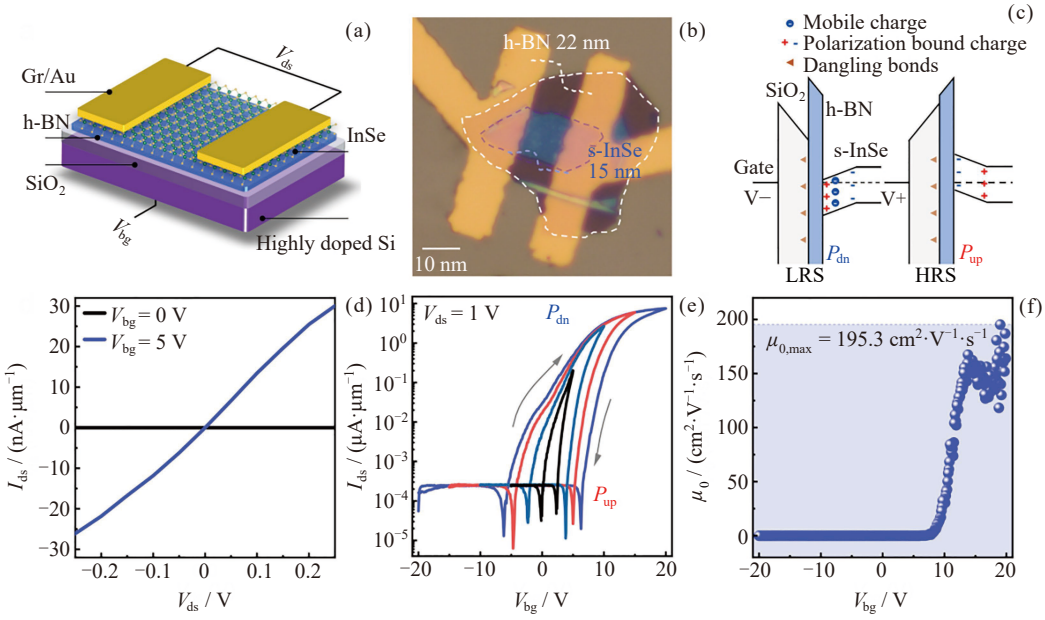


Fig. 16 Electrical performance of back-gated ferroelectric semiconductor field effect transistors[44]

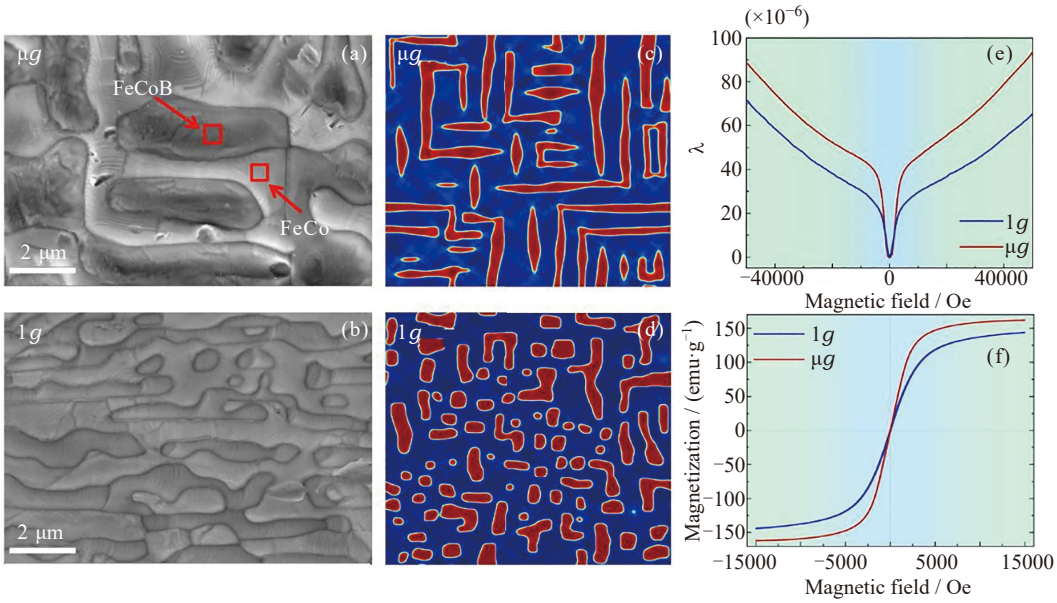


Fig. 17 Microstructures and magnetic properties of FeCoB alloys solidified in outer space and on the ground[10]

layered single crystals such as InSe, but also highlight their potential for next-generation emitter-integrated computing architectures combining memory and sensor functions.

4.4 Microstructures and Magnetic Properties of FeCoB Alloy Fabricated

FeCoB alloys were successfully fabricated by heating and melting in a containerless materials processing rack aboard the CSS. As shown in the SEM image of Figure 17(a), the phase boundaries of the sample fabricated in outer space are flat and straight, with corners tending to form right angles. In contrast, the phase boundaries of the sample fabricated on the ground are more rounded with the precipitate phase (FeCo) taking on elliptical or flow-like elongated morphologies (Figure 17b). Phase-field simulations revealed that the microgravity environment promotes higher coherent strain energy, favoring the formation of planar coherent interfaces (Figure 17c). Conversely, the reduced coherent strain energy on the ground leads to the formation of incoherent interfaces (Figure 17d).

In addition, the samples solidified under microgravity show an observable improvement in overall magnetic performance, exhibiting higher saturation magnetization along with lower coercivity. This improvement is attributed to the larger volume fraction of the FeCo precipitate phase in the outer space samples. Furthermore, coherent interfaces enable more efficient magnetoelastic coupling, resulting in superior magnetostrictive properties and higher magnetic response sensitivity, which provides a new approach for designing high-performance magnetostrictive materials.

4.5 Thermophysical Measurements of Metallic Glass-Forming Liquid

The thermophysical properties of Metallic Glass-Forming Liquids (MGFLs) are crucial for understanding glass formation and optimizing metallic glass processing. However, high-temperature metallic melts are highly reactive and easily interact with container walls, which limits the applicability of conventional contact-based measurements. In ground-based containerless experiments, terrestrial gravity makes it difficult for the sample to maintain a perfectly spherical shape, thereby significantly reducing the accuracy of thermophysical property measurements.

The microgravity environment in the Electrostatic Levitation (ESL) facility aboard the CSS provides an unprecedented opportunity for high-accuracy measurements of the thermophysical properties of high-temperature metallic melts. The research team from Shanghai University sought to measure the viscosity and surface tension of a Cu–Zr–Al MGFL aboard the CSS at temperatures inaccessible to conventional ground-based methods[45]. Figure 18(a)–(d) shows the morphological

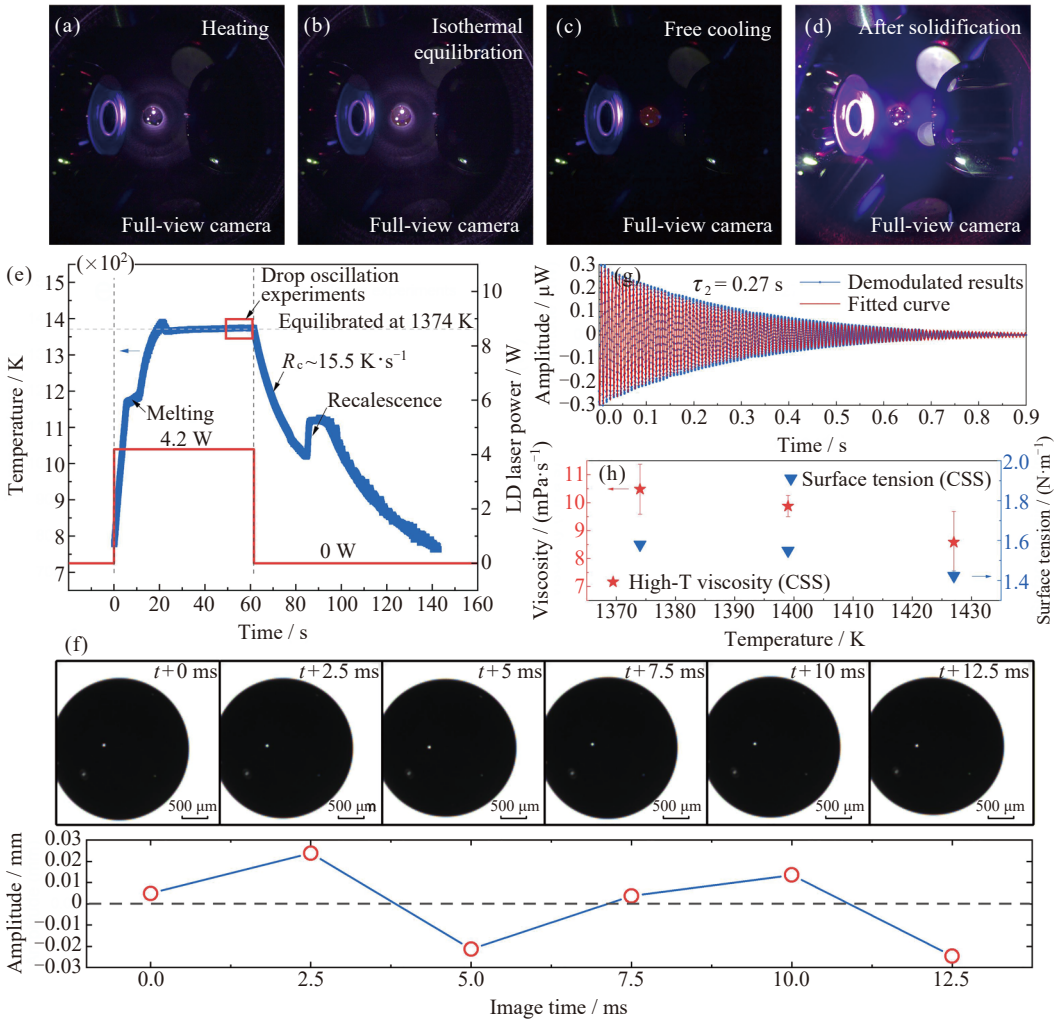


Fig. 18 On-orbit ESL experiments. (a)–(d) Full-view camera images showing the suspended sample during heating, isothermal equilibration, free cooling, and after solidification. (e) Temperature-time profile and applied laser power. (f) Images of an oscillating droplet and the corresponding oscillation amplitude. (g) Oscillation decay curve and fitted curve. (h) Temperature dependences of viscosity and surface tension[45]

evolution of a levitated sample during melting, isothermal equilibration, free cooling, and complete solidification, while the corresponding temperature profile recorded by a pyrometer is presented in Figure 18(e). Drop oscillation experiments were conducted after thermal equilibrium was reached. Figure 18(f) presents real-time images of the oscillating droplets together with the extracted oscillation amplitudes. The oscillation decay signals recorded by a photoelectric sensor are shown in Figure 18(g). The damping constant and resonance frequency were determined by fitting the decay signals and performing a fast Fourier transform, from which the viscosity and surface tension were derived (Figure 18h). Compared with contact-based Couette rheology, the viscosity data obtained aboard the CSS not only significantly extend the experimentally accessible upper temperature limit, but also eliminate anomalous viscosity signals arising from chemical reactions, demonstrating the superiority of the on-orbit containerless method for thermophysical measurements of high-temperature MGFLs.

4.6 Microgravity-Induced Suppression of Phase Segregation and Defects in Directionally Solidified $FeSe_{0.5}Te_{0.5}$ Superconductors

The mechanism by which microgravity influences the segregation of the second phase in monotectic alloys remains highly complex and urgently needs elucidation. This issue not only represents a frontier topic in solidifi-

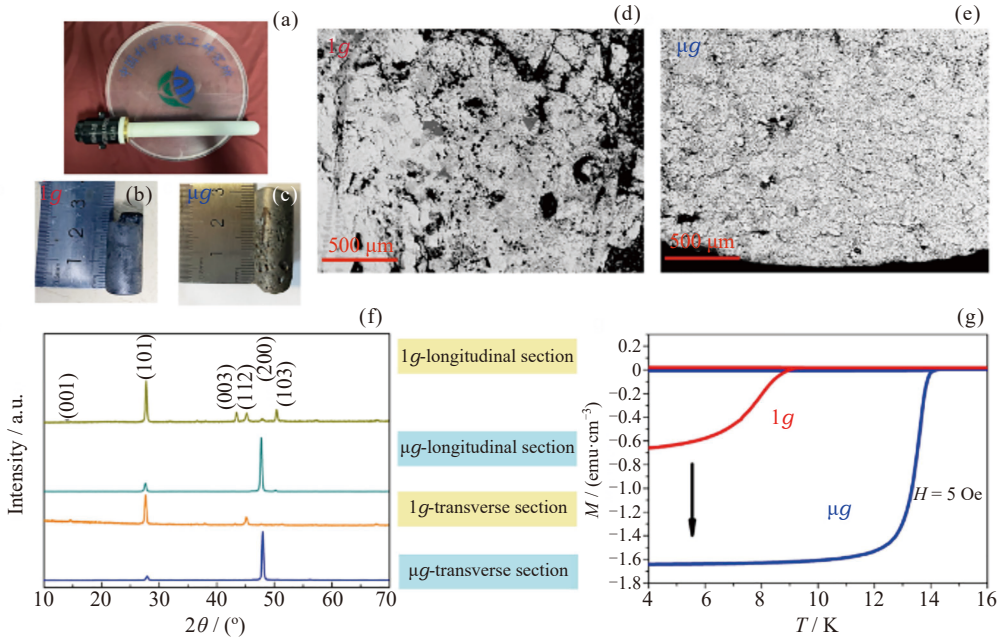


Fig. 19 Comparison of directionally solidified FeSeTe samples[10]. (a) Returned sample ampoule; (b) 1 *g* (ground) and (c) μ*g* (microgravity) sample rods; backscattered Electron (BSE) images of the (d) 1 *g* and (e) μ*g* samples, respectively; (f) XRD patterns; (g) superconducting transition

cation theory but also serves as a theoretical cornerstone for the terrestrial application of monotectic alloys. The research group at the Institute of Electrical Engineering, CAS, systematically investigated the solidification behavior of the $FeSe_{0.5}Te_{0.5}$ alloy and conducted the first microgravity experiment on iron-based superconductors aboard the CSS[46]. This study revealed the microstructure evolution and control mechanisms during space directional solidification (Figure 19a–c).

Under microgravity conditions, the absence of natural convection effectively eliminates the macro-segregation of the Se-rich phase in the liquid-liquid separation system. Concurrently, microgravity significantly weakens the crucible wall effect, suppressing the formation of stray grains induced by heterogeneous nucleation (Figure 19d, e). This promotes crystal growth along the thermal gradient direction, enabling the successful fabrication of large-sized, directionally solidified rods (3 cm in length) that are unattainable under terrestrial conditions. The texture degree, characterized by the *F*-factor, increases from 0.42 to 0.78 (Figure 19f), ultimately yielding the iron-based superconducting rod samples exhibiting strong melt texture and high compositional homogeneity. Even under rapid solidification conditions, the superconducting phase maintains an exceptionally low density of crystalline defects. This behavior is attributed to the diffusion-controlled growth regime dominant under microgravity. Microgravity markedly suppresses the formation of crystal defects during rapid directional solidification, leading to a significant reduction in interstitial iron atom density under this diffusion-dominant growth mechanism. The superconducting volume fraction of the space-processed sample exceeds twice that of its ground-based counterpart, while the superconducting transition temperature (T_c) increases from 13.2 K to 14.2 K (Figure 19g).

Space directional solidification demonstrates significant advantages in preparing FeSe-based superconductors with strong texture, high homogeneity, and superior superconducting properties. These findings open a new technological pathway to overcome the bottleneck in texture fabrication of iron-based superconducting materials. The developed preparation method is applicable to the manufacturing of high-stability superconducting magnetic bearings and maglev transportation systems.

4.7 Performance of Self-constraining PFPE Gel Lubricants

Developing highly reliable lubricating materials is critical to ensuring the stable operation of spacecraft mechanical systems and extending their service life. Perflu-

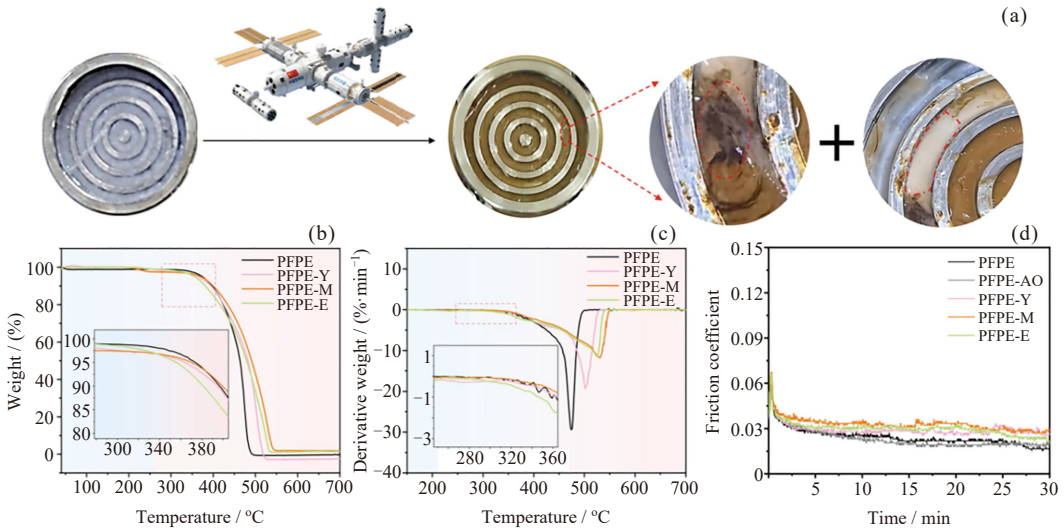


Fig. 20 Comparison of supramolecular gel before and after space exposure. (a) Photographs, (b) thermogravimetric analysis curves, (c) derivative thermogravimetric curves, (d) coefficient of friction[47]

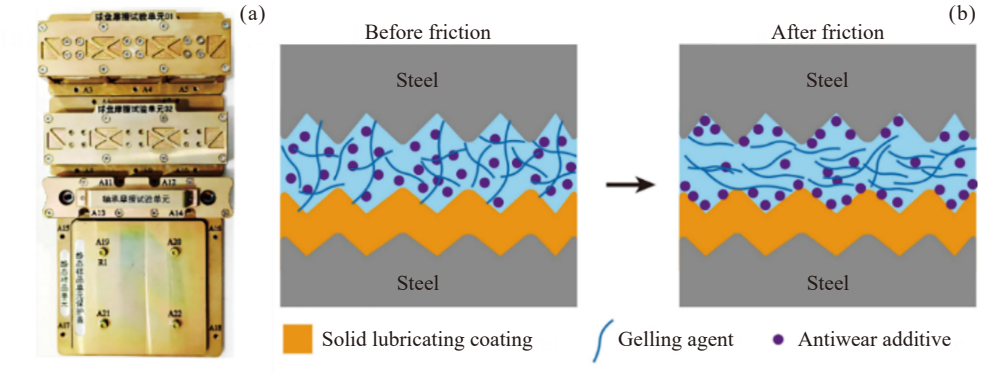


Fig. 21 Solid-liquid composite lubrication. (a) Solid-liquid composite lubrication tribology test box[10], (b) solid-liquid composite lubrication mechanism

oropolyether (PFPE) lubricants, which are the most widely used and possess excellent chemical stability, are prone to issues such as creep and migration due to their low surface tension, posing risks of lubrication failure and equipment contamination. To address this challenge, researchers at the Lanzhou Institute of Chemical Physics, CAS, have developed a self-constraint supramolecular gel lubricant by constructing a supramolecular network to confine the PFPE oil. During the first six-month extravehicular exposure experiment, the performance evolution of the gel lubricant under real space conditions (involving the synergistic effects of multiple factors) was evaluated[47]. Returned samples exhibited slight surface oxidation and discoloration due to atomic oxygen erosion, yet their internal structure remained intact (Figure 20a). Notably, compared to the original sample, the thermal stability of the exposed gel was slightly improved (the initial decomposition temperature rose from ~290℃ to ~310℃, and the maximum decomposition rate decreased from 29% min^{-1} to 11% min^{-1}), exhibiting no significant change in thixotropic properties and retaining excellent tribological performance (coefficient of friction ~0.03) (Figure 20). Investigation of the lubrication mechanism confirmed the formation of a protective tribofilm on the friction surface, composed of an adsorption layer and products of tribochemical reactions. These results indicate that this supramolecular gel lubricant possesses synergistic lubrication-sealing functions

and excellent resistance to space environment-induced coupled damage, offering a promising material solution for long-life, high-reliability aerospace applications.

4.8 Space Lubrication Experiment

Lubricating materials are essential for the normal operation of moving components in space. To address the drawbacks of current solid lubricants used in space applications (such as high friction resistance, high energy consumption, short service life) as well as the tendency of liquid lubricants to migrate and evaporate easily, a novel composite superlubrication strategy combining solid and liquid lubricants has been proposed. This approach aims to overcome the limitations of single-type lubricants. Furthermore, an extravehicular tribology experiment has been carried out using an extravehicular material exposure device equipped with a "solid-liquid composite lubrication tribology test box" (Figure 21a).

In recent experiments, four types of greases with ultra-low outgassing rates were designed to carry out ball-on-disk contact sliding tribological experiments on solid-liquid composite lubricating materials, and an extravehicular life verification of 3×10^5 revolutions was completed. Among them, some tribological properties can achieve short-term superlubrication (coefficient of friction < 0.01) or near-zero wear. Compared with the individual lubrication method, the samples based on solid-liquid composite lubrication have the lowest wear rate. In addition, novel mechanisms for achieving space superlubrication were innovatively proposed, including the shear-thinning effect and interfacial molecular absorption[48] (Figure 21b). Furthermore, the static exposure experiments of the lubricating grease revealed the mechanism of its property evolution under alternating high and low temperatures. The research results indicate that the lubrication strategy based on solid-liquid composite can effectively reduce friction and wear, with the potential to achieve "near-zero" friction and wear in space and to improve the level of space lubrication by orders of magnitude, providing new strategies for space motion equipment to achieve lower energy consumption, higher reliability, and longer operational life.

5 Microgravity Fluid and Thermal Physics

The area of microgravity fluid and thermal physics focuses primarily on a range of topics including microgravity fluid dynamics, multiphase flow and phase change heat transfer, complex fluid and soft matter, and associated applications. A body of research has been conducted on unique fluid and statistical physics phenomena under microgravity conditions. In addition, new laws of inertial particle motion in turbulent flow fields have been discovered. Furthermore, gravity mechanisms and fundamental problems have been investigated, which are difficult to delve into on the ground. Twenty-six projects (statistics as of 20 June 2026, excluding international cooperation projects) have been successfully implemented in orbit. These projects have yielded a series of significant breakthroughs in the fields of colloids crystallization, condensation heat transfer, annular flow, granular motion, among others. The progress and achievements have offered novel methodologies, technologies and systems for enhancing fluid, heat transfer and thermal management in space.

5.1 Crystallization of Charged Colloids

It is fundamentally important to study colloidal crystallization and its underlying mechanisms, as colloids are

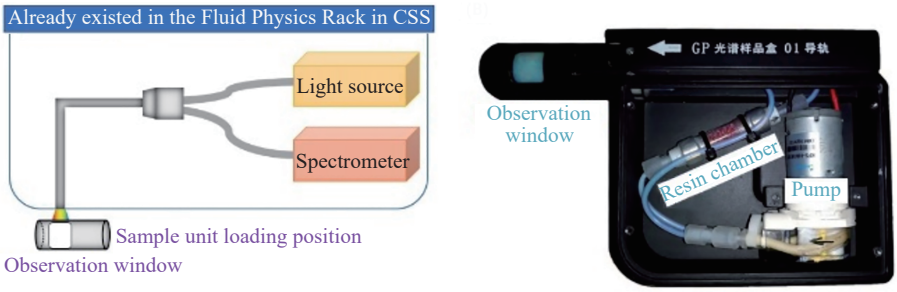


Fig. 22 Reflection spectrometer and sample unit[10,49]. (a) Reflection spectrometer in the fluid physics rack, (b) photograph of the sample unit

often regarded as "big atoms" to mimic the liquid-solid phase transition and the formed colloidal crystals are valuable materials that can be applied in various fields, such as micro- and nano-optical devices, biosensors, photonic devices, energy storage, and computer engineering. However, the effects of gravity, including sedimentation, convection and size fraction, *etc.* may significantly affect the colloids on earth, so as to make some intrinsic aspects of colloidal crystallization altered or even masked.

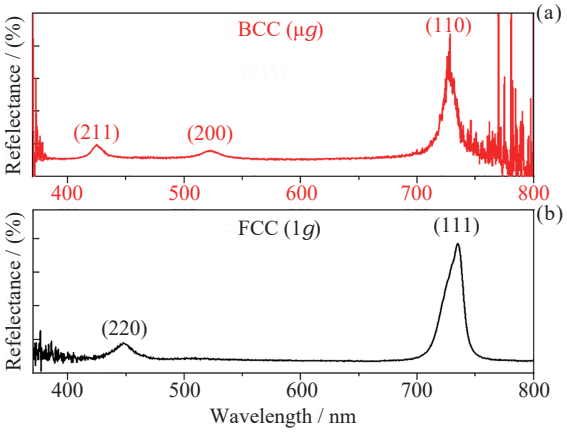


Fig. 23 Reflection spectra of colloidal crystals formed in space (a) and on the ground (b)[10,49]. The crystal structures are metastable BCC and stable FCC, respectively

With respect to the mechanism of colloidal crystallization, both experiments and numerical simulations have shown that the crystal nucleation is not a one-step process as described in the framework of Classic Nucleation Theory (CNT), but rather a two or even multi-step process. For the charged colloids, whose effective interactions based on DLVO (Derjaguin, Landau, Verwey, and Overbeek) theory can be tuned relatively freely, we have recently investigated its crystallization using the reflection spectrometer in the CSS (see Figure 22). The colloidal sample, which exhibits a thermodynamically stable Face-Centered Cubic (FCC) phase in normal gravity, manifests a long-lived metastable Body-Centered Cubic (BCC) phase under microgravity (see Figure 23). The simulation of molecular dynamics is in agreement with the observations of space experiment, as it also shows the formation of metastable BCC crystals. Furthermore, the free-energy calculations suggest that BCC-FCC transition cannot be fully realized within the temporal confines of the space experiment. Those findings not only demonstrate Ostwald's step rule and Alexander-McTague argument specifically for charged colloidal

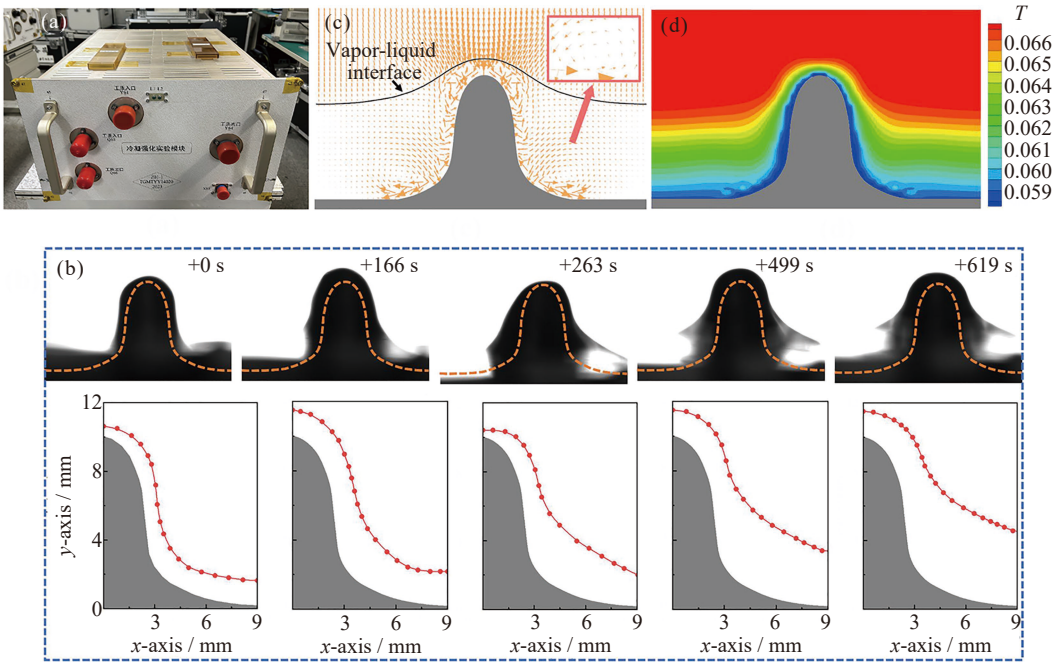


Fig. 24 Evolution behavior and heat transfer of the space condensation liquid film on a single pin-fin surface[10]. (a) Experimental setup for film condensation under microgravity, (b) evolution of the condensation interface on the single pin-fin surface under microgravity, (c) velocity field distribution, (d) temperature distribution

systems where the metastable BCC crystals are formed, but also provide further evidence that gravity effects may play a substantial role in promoting the BCC-FCC transition.

5.2 Film Condensation Heat Transfer on Single Pin-Fin Structure Surface

To elucidate the effects of microgravity on film condensation behavior on a single pin-fin surface, the Southeast University research team previously conducted experiments and multi-scale numerical simulations on ground and in the falling tower[50–52]. To obtain the complete evolution process of the liquid film from formation to spreading on a single pin-fin surface under long-term microgravity, the team conducted film condensation experiments using HFE-7100 as the working fluid on the single pin-fin surface aboard the CSS (Figure 24a). As shown in Figure 24b, under microgravity conditions, the condensate film does not spread uniformly; instead, it accumulates at the base of the pin-fin and gradually extends outward, leading to a significant reduction in heat transfer performance. Compared with the terrestrial gravitational environment, gravitational drainage is considerably weakened under microgravity, resulting in a prolonged residence time of the liquid film at the pin-fin base and the formation of a thicker local liquid film layer. This phenomenon increases the thermal resistance at the condensation interface and substantially degrades the overall heat transfer performance. Figure 24(c)(d) illustrate the characteristics of the velocity field and surface temperature distribution during the evolution of the condensation interface. It is evident that a temperature non-uniformity exists along the height direction of the pin-fin, which enhances the surface tension gradient and thus induces strong thermocapillary convection (Marangoni effect). Thermocapillary convection promotes micro-convection within the liquid film and intensifies interfacial fluctuations, thereby improving, to some extent, the condensation heat transfer performance under microgravity. This result indicates that, although the absence of gravitational drainage deteriorates heat transfer in the microgravity environment, the thermocapillary effect driven by temperature non-uniformity may serve as a beneficial compensatory mechanism. This study enriches the stability theory of microgravity condensation liquid films and provides support for the design of two-phase thermal management systems in future space exploration.

5.3 Oscillation and Transition Characteristics of Microgravity Annular Flow

Thermocapillary convection, driven by the variation of

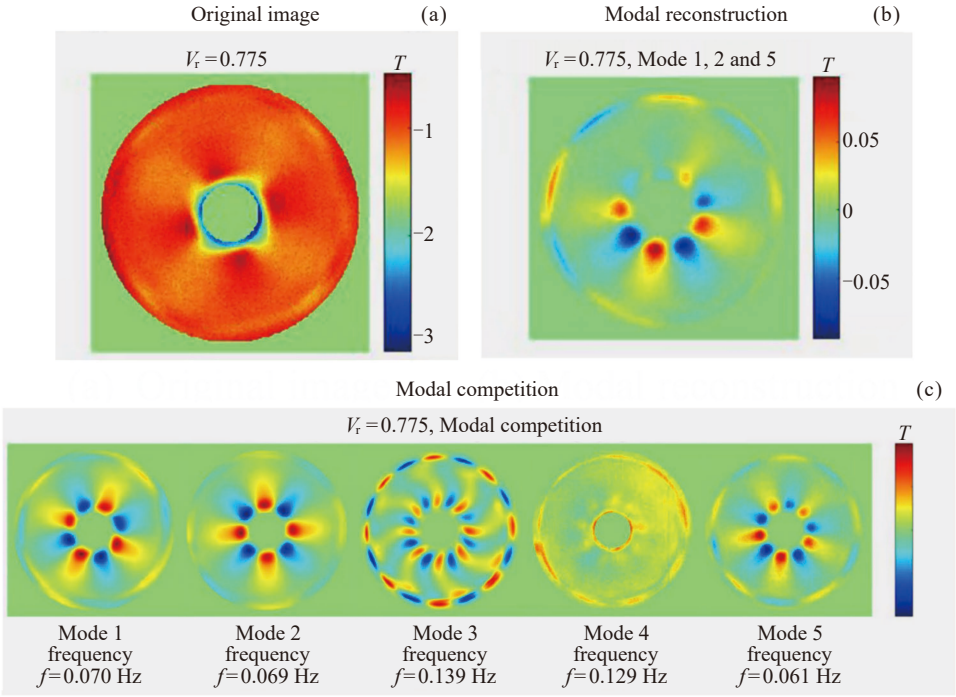


Fig. 25 Modal competition of thermal fluid waves under microgravity annular flow[6]

the free surface tension of fluids with temperature gradients, is a typical nonlinear flow. It plays an irreplaceably critical role in applications such as microgravity material crystal growth, spacecraft thermal management, chip cooling, and microfluidic device design. Among these applications, the study of thermocapillary convection under microgravity annular flow scenarios is particularly significant. The stability and oscillatory characteristics of its flow modes directly affect the morphology of crystal growth interfaces, heat and mass transfer efficiency, and the operational performance of microdevices, thus becoming a research focus in the interdisciplinary field of fluid mechanics and engineering thermophysics.

An annular flow system with three fully controllable parameters—fixed central cylinder, rotating central cylinder, and lifted central cylinder—has been established in the microgravity environment[53]. We discovered the critical jump phenomenon of hydrothermal waves affected by the volume ratio effect, verified the universality of this effect, and revealed the intrinsic nature of the instability steps of high-frequency and low-frequency waves. Additionally, we obtained the multimodal evolution and competitive propagation laws of hydrothermal waves in the supercritical regime, including Standing Waves (SW), Traveling Waves (TW), linear waves, and chaotic waves[6](Figure 25), which exhibit strong nonlinear effects[54]. Forced convection (Taylor-Couette flow) was introduced to regulate thermal convection, ultimately achieving the control of the quasi-equilibrium state of the flow.

These findings deepen the understanding of thermal convection turbulence dominated by surface forces in space environments, provide guidance for the selection of key parameters for high-quality crystal growth, and offer theoretical support for industrial crystal growth practices.

5.4 Influence of the Friction Coefficient on the Motion of Dry Granular Materials in Variable Gravity Environments

The systematic investigation of the influence of friction is provided on the motion of dry granular materials across gravity fields ranging from 0.01 g to 1 g[55–57]. By eliminating inter-particle cohesion and electrostatic forces, the study examines this behavior from two complementary perspectives: the dynamic and static angles of repose (Figure 26a), and the segregation dynamics of particles with differing sizes (Figure 26b). In Compartment A, observations of quasi-static and free-collapse pile angles revealed that the static angle of repose is independent of gravity level, whereas the dynamic angle of repose decreases markedly below lunar gravity (≈0.165 g). In Compartment B, experiments tracking the upward migration of a single large particle in a vibrating granular bed showed that higher vibration accelerations are required to initiate movement under reduced gravity — an effect that becomes pronounced only below lunar gravity[57] (Figure 27). Collectively, these findings demonstrate that the static friction coefficient remains essentially unchanged with gravity, while the rolling friction coefficient is a function of gravitational acceleration. Consequently, particle resistance to sliding stays stable across Earth, lunar, and asteroid environments, yet weaker gravity markedly facilitates rolling, flow, and reorganization. This enhanced granular fluidity in microgravity environments significantly increases the susceptibility of asteroid surface materials to deformation, loosening, rotational instability, and local collapse.

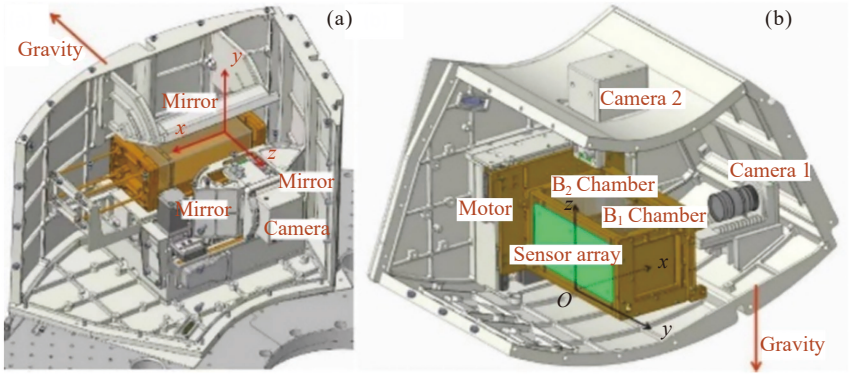


Fig. 26 Setup diagram of the CSS granular fluidization experiments for Chamber A (a) and Chamber B (b)[6]

6 Microgravity Combustion Science

The area of microgravity combustion science focuses primarily on the investigations of the near-limit flammability and their underlying physics, critical combustion mechanisms, and applied research, material ignition characteristics and protective measures under microgravity, *etc*. Thirteen projects (statistics as of 20 June 2026) have been successfully implemented in orbit, and a series of discoveries and breakthroughs have been achieved in basic combustion processes and mechanisms. These include multi-jet diffusion flames, soot production, and near-limit partially premixed flames, among others. The progress and achievements have yielded novel findings and insights relevant to the technological development, including low-carbon combustion, advanced power, and efficient clean energy, *etc*.

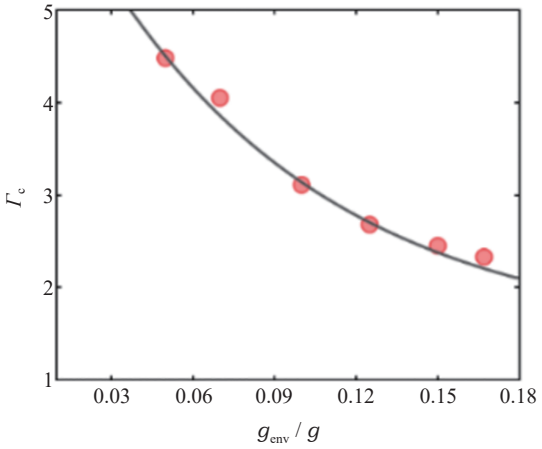


Fig. 27 Critical vibration acceleration required for large particles to move upwards decreases as gravity increases

6.1 Research on Multi-jet Diffusion Flames

Leveraging the Gaseous Combustion Experiment Insert (GCEI) aboard the CSS, this study developed a multi-jet combustion assembly tailored for orbital environments. By integrating high-resolution imaging with advanced optical diagnostics, we achieved the precise observations of flame morphology, temperature distributions, and radiative intensities of methane multi-jet flames under microgravity. The results reveal that the suppression of buoyancy-induced convection leads to a highly symmetric and stable flame structure, where inter-jet interactions are primarily governed by momentum flux and

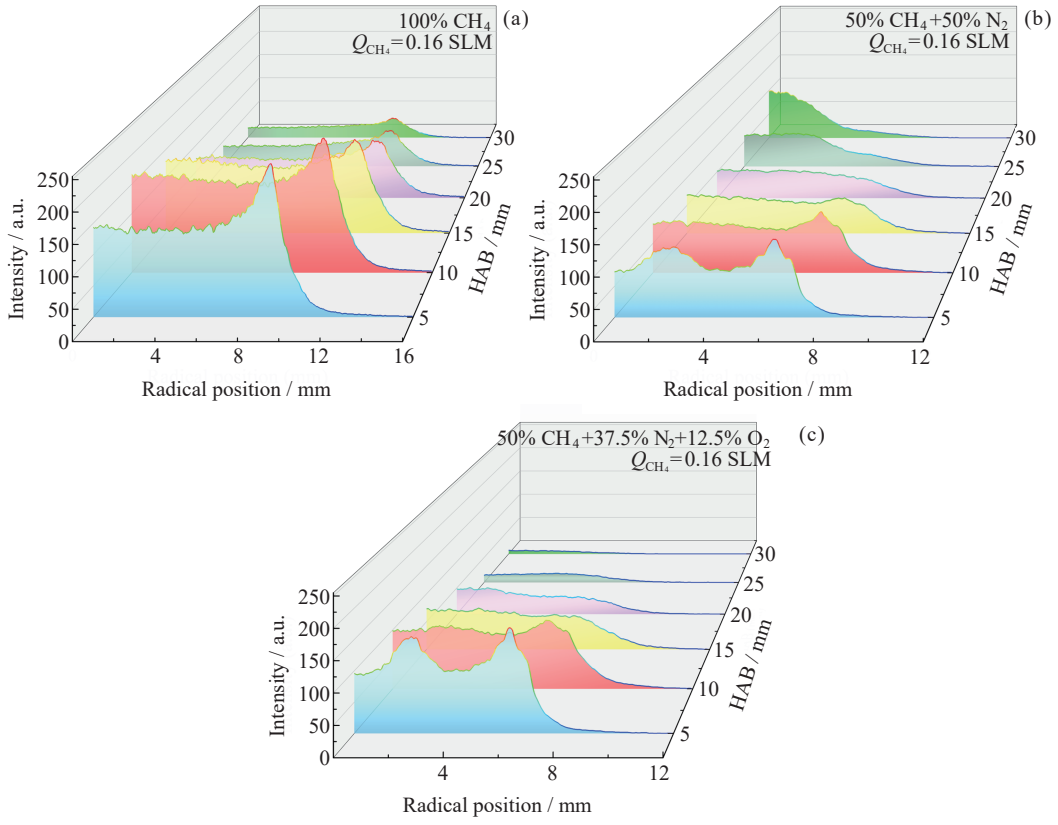


Fig. 28 CH* radical intensity with radial position at different heights of the flames

molecular diffusion, resulting in a distinct reaction zone distribution[58].

Critically, a significant enhancement in flame radiation under microgravity was observed. The coupling between fuel jets and soot evolution was found to be dual-faceted: intensified high-temperature zones at elevated flow rates accelerate soot inception, whereas enhanced mixing in the diffusion-dominated regions promotes oxidation, thereby suppressing soot emissions[59]. Numerical simulations—incorporating reduced chemical kinetics, radiative heat transfer, and semi-empirical soot models—demonstrate that multi-jet coupling fundamentally alters precursor distributions and reaction pathways, which dictates the spatial characteristics of pollutants. Furthermore, the study characterizes the influence of fuel blending on flame merging behavior under microgravity as shown in Figure 28, providing a foundational theoretical framework for spacecraft fire safety and combustion control.

6.2 Soot Production in Non-buoyant Laminar Diffusion Flames

Soot represents one of the fundamental topics in combustion and fire research. Experiments with non-buoyant laminar diffusion flames are crucial for both elucidating the soot processes and providing more tractable model systems that are relevant to turbulent flames. A series of microgravity experiments has been performed to investigate soot properties of laminar diffusion flames aboard the CSS. Axisymmetric jet flames in coflowing oxidizer stream were tested, and hundreds of diffusion flames were recorded at various conditions. The experimental conditions included pure methane, nitrogen- or argon-diluted fuel, air coflow, and nitrogen- or argon-diluted coflow.

According to extracted data, the volume fraction of the inert dilution gas and the flame temperature are recommended to characterize the dilution and thermal effects on soot production, respectively. With a diluted coflow, comparing to the undiluted case, the region where soot formation is more prevailed over soot oxidation decreases in height, while the oxidation-dominated region expands simultaneously. The observed trend continues as the dilution gas increases, resulting in the decrease of the overall soot concentration and the maximum soot load in the diffusion flame[10,60] (Figure 29). Hydrodynamic effects on the soot processes are revealed under the research context, and a correlation model for smoke point is proposed to explicitly consider the apparent effects of jet outlet diameter and coflow magnitude[61].

6.3 Liftoff Stabilization and Extinction Behaviors of Near-limit Partially Premixed Flame

As the first series of combustion experiments aboard the CSS, transient extinction and stabilization of partially premixed methane-air flames were conducted using a co-flow jet burner (Figure 30) within the Gas Combustion Experiment Insert (GCEI) [62]. The investigations systematically varied jet velocity, equivalence ratio, and dilution (N_2, Ar) to independently examine the effect of

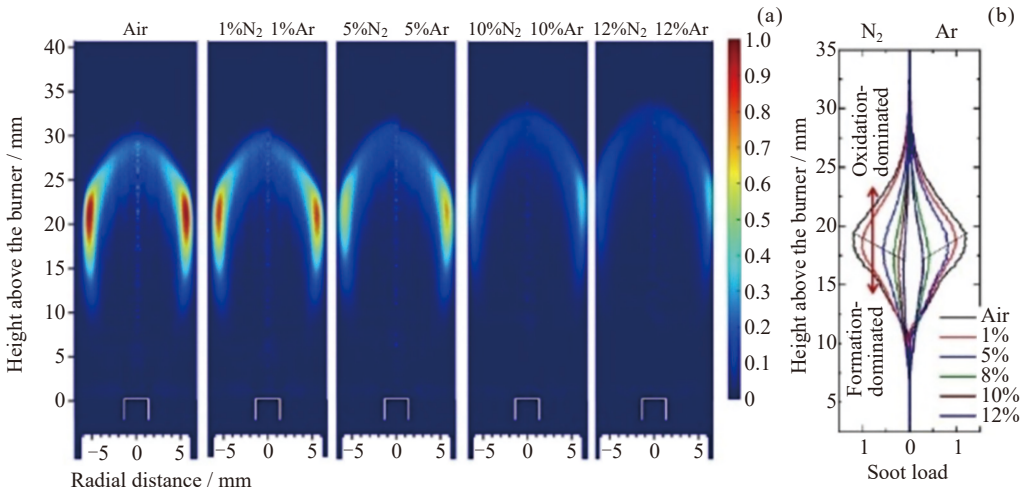


Fig. 29 Soot concentration distributions (a) and evolution of soot load (b) under microgravity laminar diffusion flames at various coflowing oxidizer conditions[10,60]

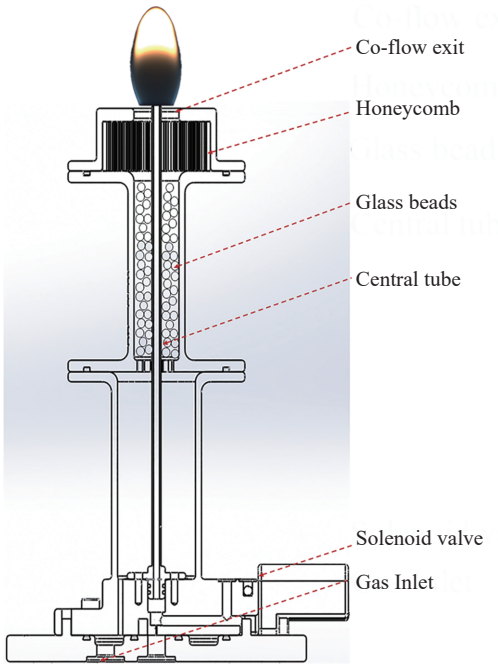


Fig. 30 Burner configuration

Damkohler and Markstein numbers on the flame stabilization and extinction. Contribution of radiation to the extinction behaviors was analyzed using MultiDiff-FOAM simulations[63]. Flames with identical conditions under 1 g and μg[10] (Figure 31a) suggest significant differences and hence highlight the necessity of experiments under microgravity.

Aerodynamic strain and flame curvature effects were separately studied for macroscopic flame liftoff. It was found that liftoff height correlates with the inverse mixing Damköhler number (Da_m^{-1}) (Figure 31b), which effectively links macroscopic flow timescales to microscopic stretch dynamics. Markstein numbers for curvature (Ma_c) and flow strain (Ma_s) were calculated along the flame. Results revealed that curvature-induced stretch dominates over strain ($|Ma_c| > |Ma_s|$) on the flame globally, and presence of gravity suppresses curvature while enhancing strain while Ar amplifies curvature sensitivity. By quantitatively separating the competing effects of radiation, strain, and curvature in a buoyancy-free environment, this research provides a physically in-

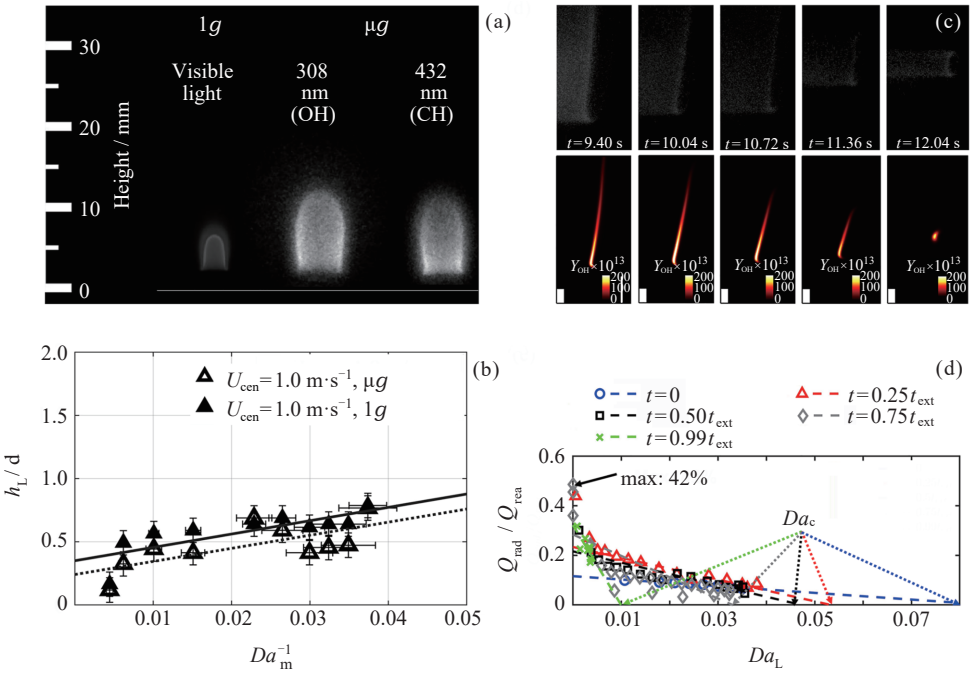


Fig. 31 Lift-off stabilization and extinction behaviors of near-limit partially premixed flame under microgravity[6,10]. (a) Lift-off flame in 1 g and μg, (b) flame liftoff height h_L over burner size d, *i.e.*, h_L/d *vs*. inverse of mixing Damköhler number Da_m^{-1}, (c) extinction of partially premixed flame under microgravity (upper: experiment; lower: simulation), (d) analysis from simulation for Q_{rad}/Q_{rea} (radiative heat loss over total reaction heat release) *vs*. Damköhler number Da_L

terpretable framework and critical data for refining combustion models.

Under some near-limit conditions[6] (Figure 31c), the Non-Premixed Flame (NPF) branch of a partially premixed flame exhibits a ring-like structure with partially premixed hooks prior to global extinction[64]. In such a newly observed behavior, radiative heat loss occupied up to 40% of local heat release at the NPF edges[6] (Figure 31d). These flame edges retract in a premixed manner, shifting the local extinction mechanism from strain-controlled to radiation-controlled, which ultimately triggers the extinction of the entire NPF region.

7 Microgravity Fundamental Physics

The area of microgravity fundamental physics focuses primarily on space cold atom physics, high-precision time-frequency and related fundamental physics, microgravity plasma physics, *etc*. Five projects (statistics as of 20 June 2026) have been successfully implemented in orbit. A series of significant breakthroughs have been achieved in the fields of cold atom physics, interferometer, and others in space. Current breakthroughs lay a foundation for ongoing research, with studies continuing to ultra-low temperature quantum states, ultra-cold optical lattice quantum simulations, high-precision atomic clocks and time-frequency transmission technology. The progress and achievements made in these fields will be applied to fundamental physics theory testing and navigation timing.

7.1 Space Cold Atom Interferometer for Inertial Sensing

Cold Atom Interferometers (CAIs) can measure absolute acceleration and rotation with high precision. Benefiting from long interrogation time under microgravity, the inertial measurement precision of CAIs is significantly enhanced, making space CAIs an important candidate for high-precision inertial sensors in space. We developed a highly integrated optical architecture for the CSS Atom Interferometer (CSSAI). The scheme uses only two seed lasers, one tapered amplifier, and one acousto-optic modulator to generate all required frequencies for cooling, state preparation, Raman transitions, and detection. A fused silica optical bench with double-sided bonding minimizes thermal deformation, while silicone vibration isolators protect the bench during launch. The assembled optics measures 250 mm×240 mm×104 mm and weighs 5.2 kg, the most compact space CAI optics to date (Figure 32). Launched to the CSS in 2022, the system has operated reliably for over two years with-

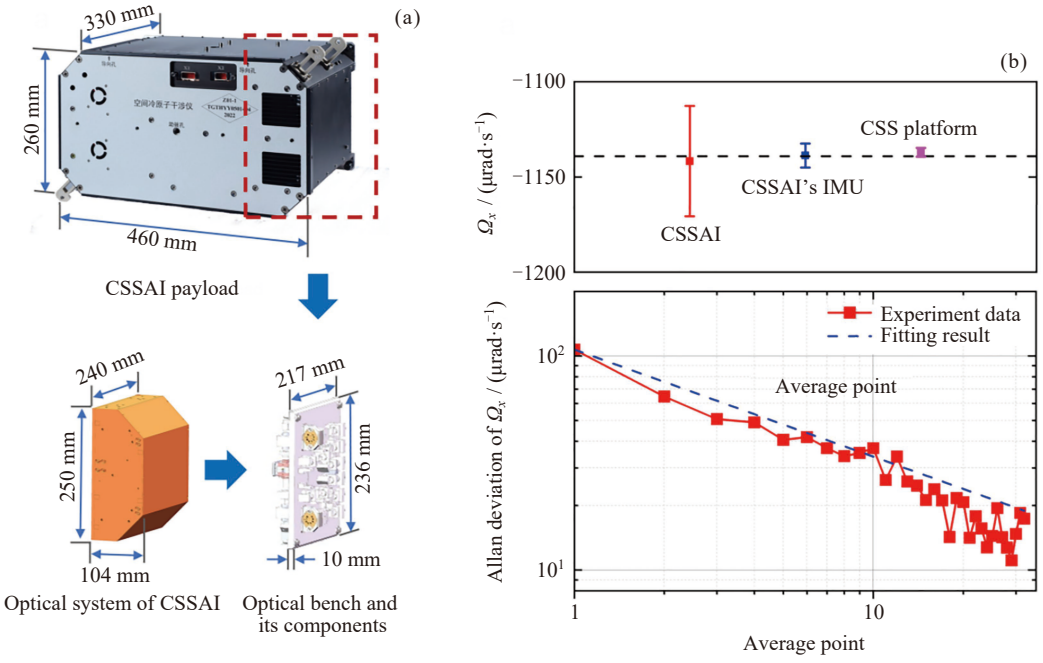


Fig. 32 CSSAI and rotation measurement. (a) CSSAI and its optical system[6], (b) rotation measurement in space

out manual tuning. Output laser power fluctuations remain below 2.5% over months, and frequency stability stays better than 1 MHz[65].

For inertial measurement, the CSSAI performed on-orbit characterization under the station's high-dynamic rotation (about 15 times Earth's rate). A closed-loop two-axis piezoelectric mirror cancels the angular motion, enabling point-source interferometry. With 75 ms interrogation time, the gyroscope achieves a rotation resolution of 50 μrad·s^{-1} per shot and 17 μrad·s^{-1} after averaging 32 shots. The measured orbital rotation rate is (−1142±29) μrad·s^{-1}, agreeing with the CSS platform's classical gyroscope (−1137.0±2.3) μrad·s^{-1}. The same interferometer simultaneously measures linear acceleration with a single-shot resolution of 1.0 μm·s^{-2}, demonstrating a standalone quantum inertial measurement unit[66] (Figure 32).

7.2 Realization of Laser Cooling Alkaline-Earth Atom under Microgravity

Relying on the strontium optical clock payload aboard the CSS, laser cooling of alkaline-earth atoms was achieved in a space microgravity environment[67]. This successfully expands the capability boundary of cold-atom physics experiments under the extreme conditions of microgravity, representing a landmark advancement in the space-based cold-atom physics experimental technologies in China. Alkaline-Earth elements such as strontium possess a dual-valence-electron structure with singlet and triplet states, making their laser cooling more complex in optical configuration and control logic than alkali-metal systems and imposing higher technical demands. The project team developed a highly integrated miniaturized space strontium optical clock physics system, overcoming challenges in the miniaturization and vibration resistance of sophisticated opto-mechatronic systems. The system integrates more than ten high-stability lasers and achieved on-orbit frequency locking for each laser beam[68]. Having successfully endured the rigors of rocket launch and the on-orbit environment, the system has operated stably over extended periods, realizing the laser cooling of both strontium isotopes, ^{87}Sr and ^{88}Sr, under microgravity conditions (Figure 33). Cameras inside the optical clock system clearly captured images of laser-cooled strontium cold-atom clouds in a magneto-optical trap, verifying the effective implementation of laser cooling.

The accomplishment of on-orbit laser cooling (first-stage cooling) of alkaline-earth strontium atoms lays a solid technical foundation for the operation of high-performance space optical clocks. This breakthrough not only expands the frontier of microgravity cold-atom physics, but also strongly advances China's establishment of an independent, world-leading, space-ground in-

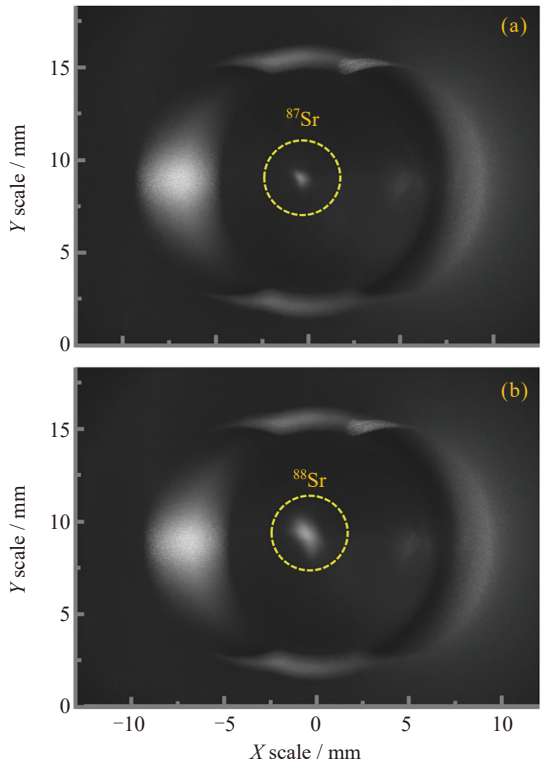


Fig. 33 Magneto Optical Trap (MOT) atoms photography shot by the CCD camera[67]. (a) ^{87}Sr MOT atoms, (b) ^{88}Sr MOT atoms

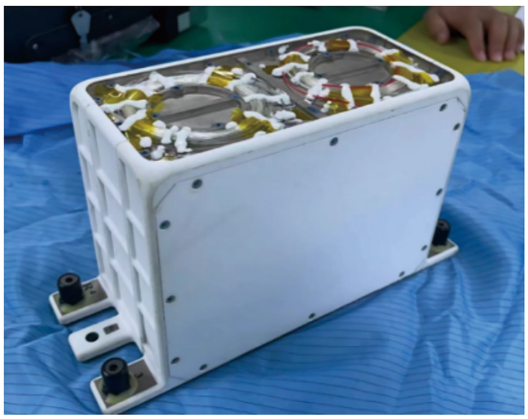


Fig. 34 Experiment unit and fiber optic irradiation sensors[10]

tegrated high-precision time-frequency system. It provides crucial support and assurance for major future needs, including next-generation satellite navigation, deep-space exploration, tests of general relativity, and even future gravitational-wave detection.

8 Space Innovative Technology Demonstration

The area of space innovative technology demonstration focuses primarily on the space effect mechanism of components and assemblies, space information and precision measurement, *etc*. Fifteen projects (statistics as of 20 June 2026) have been successfully implemented in orbit. Valuable mechanisms of space effects have been acquired, and a series of key technology breakthroughs have been accomplished on high-performance, complex, and new electronic components and sensors. Some of these technologies have been promoted and transitioned into the aerospace technology and other fields. The field is dedicated to the demonstration and transformation of high-precision space detection and measurement technologies.

Example of progress: verification of key performance parameters for fiber optic sensors. The anti-radiation fiber grating temperature sensor is fabricated by femtosecond laser engraving method[69]. The measurement range of the sensor is –65℃ to 135℃, and the temperature measurement accuracy is 0.1℃. In addition, according to the performance characteristics of the irradiation sensitive optical fiber, the high sensitive optical fiber is selected to make the optical fiber irradiation sensor[70] (Figure 34). The experiment verifies the reliability of the design of the new optical fiber sensor, and tests the performance and life of the optical fiber sensing system under the coupling environment of complex factors such as space irradiation, single particle and atomic oxygen under the long-term on-orbit working state[71]. The results provide technical support for the application of optical fiber sensing technology in orbit.

9 International Cooperations

We have gradually promoted the establishment of a broad and multi-level international cooperation network, including major foreign space agencies such as ESA, DLR, CNES, SUPARCO, EGSA, SSA, SSO, ASI, as well as important international space organizations, including UNOOSA, UNESCO, IAF, COSPAR, MVA. We have also engaged in comprehensive and systematic international cooperation with universities and research institutions.

In recent years, by comprehensively utilizing flight resources such as Shenzhou spacecraft, Tiangong laboratory, the CSS, the International Space Station, some scientific satellites, parabolic aircraft and sounding rockets, China has carried out joint research and development of scientific experiment payloads with foreign partners and supported Chinese and foreign scientific teams in conducting scientific research and academic exchanges. A large number of valuable scientific research achievements have been made. Nearly 40 joint experiments have been successfully carried out, and more than 20 international cooperation projects are being cultivated, demonstrated and implemented. A demonstration effect has been initially achieved. International mega science program is also in plan.

10 Summary

The science and utilization mission has been executed in an efficient manner, and the advanced experiments conducted aboard the CSS have revealed a series of novel scientific phenomena and laws under space conditions in diverse areas, including life sciences, materials science, fluid physics, combustion, and cold atom physics, *etc*. A series of research models have been developed, and a range of key technology breakthroughs have been achieved, including space animal cultivation, the preparation of important crystal materials, fluid and thermal management, space cold atom interferometer, and on-orbit combustion experimental technologies. In addition, applications and transformations have been initially attempted. Two annual progress reports (in 2024 and 2025) had been released, which cover a substantial array of achievements across multiple areas. Therefore, the progress greatly advance the development of space science, utilization, and technology in China.

In the future, science and utilization projects will be dynamically solicited and selected on a continuous implementation basis. Meanwhile a series of management policies will be gradually established for the projects.

According to the plan, nearly a thousand projects will be implemented. These projects will focus on the frontiers of science and technology, serve national strategic needs, and call on more high-level experts and teams to actively participate in the CSS science and utilization research.

Acknowledgements We would like to express sincere gratitude to the CMSA for its organization and leadership, and sincerely thank all the project teams for their guidance and help, including: Wang Hongmei, Zheng Weibo, Li Tianda, Li Yan, Zhen Huiqiong, Long Mian, Li Ning, Ying Hao, Li Yuying, Zhang Chunling, Chen Yutao, Zhao Yufen, Liu Yan, Sun Yeqing, Zhao Lei, Wei Bingbo, Wang Haipeng, Liu Xuechao, Yu Jianding, Jin Min, Yang Sen, Wang Yu, Wang Gang, Ma Yanwei, Dong Chiheng, Tang Minghui, Zhou Feng, Cai Meirong, Wang Daoai, Zhan Mingsheng, Chen Xi, Chang Hong, Xu Shenghua, Chen Zhenqian, Xu Bo, Duan Li, Kang Qi, Hou Meiying, Tian Zhenyu, Wang Shuangfeng, Zhang Yang, Liu Yucheng, Zhu Lianqing, Li Shengyang, Liu Kang, Zhao Guoping, Cai Ronggen, He Guowei, Yao Qiang as well as other related colleagues in general establishment of space science and utilization, including Zhang Lu, Zhao Liping, Gong Yongsheng, He Yufeng, Ma Ping, Guo Xiaoxiao, Du Changshuai, Han Pei, Zhang Yingyi, Liu Yan, Wang Chong, Feng Xuan, Jiao Jian, Han Yuexia, *etc*.

Conflict of Interests The authors declare that there is no conflict of interests

References

[1] ZHOU J P. Chinese Space Station Project Overall Vision[J]. *Manned Spaceflight*, 2013, **19**(2): 1-10 (in Chinese)

[2] WANG X, WANG W. Key technical characteristics of the Tiangong Space Station[J]. *SCIENTIA SINICA Technologica*, 2021, **51**: 1287-1298. (in Chinese)

[3] GU Y D. The China Space Station: a new opportunity for space science[J]. *National Science Review*, 2022, **9**: nwab219

[4] GU Y D, GAO M, ZHAO G H. Space research plan of China's Space Station[J]. *Chinese Journal of Space Science*, 2016, **36**(05): 595-599

[5] GU Y D, GAO M, ZHAO G H. Science research and utilization planning of China's Space Station in operation period 2022—2032[J]. *Chinese Journal of Space Science*, 2020, **40**(5): 609-614

[6] China Manned Space Agency. Report on Scientific Research and Application Progress of the China Space Station (2024) [EB/OL]. 2024-12-30 [2026-04-30]. https://www.cmse.gov.cn/xwzx/202412/W020241231661310955564.pdf (in Chinese)

[7] YAN Gong, MIAO Haitao, ZHAN Hu, *et al*. Introduction to the Chinese Space Station Survey Telescope (CSST) [J]. SCIENCE CHINA Physics, Mechanics & Astronomy, 2026, **69**(3): 239501. DOI: 10.1007/s11433-025-2809-0

[8] ZHANG S N, DONG Y W, GAO X H, *et al*. The High Energy Cosmic-Radiation Detection (HERD) facility in space[J]. *Manned Spaceflight*, 2015, **21**(1): 69-74

[9] China Manned Space Agency, Press conference held for the Shenzhou-17 manned space mission [EB/OL]. CMSA. 2023-10-25[2026-05-12]. https://www.cmse.gov.cn/xwzx/202310/t20231025_54498.html (in Chinese)

[10] China Manned Space Agency. Report on Scientific Research and Application Progress of the China Space Station (2025) [EB/OL]. 2026-01-08 [2026-04-30]. https://www.cmse.gov.cn/xwzx/202601/W020260108444152803150.pdf (in Chinese)

[11] GU Y D, GAO M, ZHAO G H, *et al*. Recent progress in space science and applications on Chinese Space Station in 2022-2024[J]. *Chinese Journal of Space Science*, 2024, **44**(4): 607-621

[12] YUAN R, SUN H Y, ZHANG Q, *et al*. Gas purification technology suitable for space mice cultured in sealed box[J]. *Processes*, 2025, **13**(10): 3277

[13] CAIN J C, FERGUSON B B, MOZZONI D. An n = 90 internal potential function of the Martian crustal magnetic field[J]. *Journal of Geophysical Research Planets*, 2003, **108**: 1-19

[14] SINČÁK M, SEDLAKOVA-KADUKOVA J. Hypomagnetic fields and their multilevel effects on living organisms[J]. *Processes*, 2023, **11**(1): 282

[15] BERGUIG M S, HAMOUDI M, LEMOUËL J L, *et al*. Validate global mapping of internal lunar magnetic field[J]. *Arabian Journal of Geosciences*, 2011, **6**: 1063-1072

[16] LI S Y, LIU K, WANG H, *et al*. Pose estimation and tracking dataset for multi-animal behavior analysis on the China Space Station[J]. *Scientific Data*, 2025, **12**(1): 766

[17] ZHOU Z, LI S Y, LV Y X, *et al*. A deep learning framework for multi-object tracking in space animal behavior studies[J]. *Animals*, 2025, **15**(16): 2448

[18] LIU K, LI S Y, LV Y X, *et al*. Structure-aware multi-animal pose estimation for space model organism behavior analysis[J]. *Animals*, 2025, **15**(21): 3139

[19] XIE J Y, ZHU J C, WANG L H, *et al*. Potential regulatory modules to integrate microgravity signals into flowering pathways in Arabidopsis thaliana grown in space[J]. *ResearchGate*, 2025, **11**: 87. DOI:10.1038/s41526-025-00539-z

[20] XIE J Y, WANG L H, ZHENG H Q. Molecular basis to integrate microgravity signals into the photoperiodic flowering pathway in Arabidopsis thaliana under spaceflight condition[J]. *International Journal of Molecular Sciences*, 2022, **21**(1): 63. DOI:10.3390/ijms23010063

[21] WANG L H, XIE J Y, MOU C H, *et al*. Transcriptomic analysis of the interaction between FLOWERING LOCUS T induction and photoperiodic signaling in response to space flight[J]. *Frontiers in Cell and Developmental Biology*, 2022, **9**: 813246

[22] JIA C X, ZHENG W B, LIU F W, *et al*. Biological culture module for plant research from seed-to-seed on the Chinese Space Station[J]. *Life Science in Space Research*, 2024, **42**: 47-52

[23] WU Y Y, XIE J Y, WANG L H, *et al*. Circumnutations and growth of inflorescence stems of Arabidopsis thaliana in response to microgravity under different photoperiod conditions[J]. *Life* (*Basel*), 2020, **10**(3): 26

[24] LI N, ZHANG X Y, LUO H, *et al*. Shear flow alleviates spaceflight-induced hepatic lipid dysregulation via suppression of SREBP mechanotransduction [J]. *Science Bulletin*, 2026. DOI: 10.1016/j.scib.2026.01.072

[25] LI Y, XUE L M, WANG F J, *et al*. , Lactylation of mTOR enhances autophagy in skeletal muscle during exercise[J]. *Cell Chemical Biology*, 2025. **32**(11): 1367-1380 e5. DOI: 10.1016/j.chembiol.2025.10.007

[26] KONG W Q, MA M, LI Z Y, *et al*. Comprehensive analysis of miRNA expression, secretion profile, and functional network during myogenesis in response to spaceflight[J]. *NPJ Microgravity*, 2026, DOI: 10.1038/s41526-026-00632-x

[27] NIU Z M, YAN Y, LIU W, *et al*. Aberrant miR-378 expression promotes hepatic lipid accumulation via hijacking the bile acid-regulated autophagy[J]. *Life Metabolism*, 2026, **5**(1): loaf038

[28] MA M, MA R S, LI Z Y, *et al*. NAD+ subcellular partitioning mediated by miR-183 and miR-96 regulates muscle stem cell differentiation[J]. *Journal Molecular Cell Biology*, 2026, mjag015

[29] LI Z Y, MA M, MA R S, *et al*. , MRG15 decline in aged/injured MuSCs hinders regeneration via differentiation defects[J]. *Cell Regeneration*, 2026, **15**(1): 8

[30] XIN Y H, XIAN R Q, YANG Y G, *et al*. Structural and functional insights into the T-even type bacteriophage topoisomerase II[J]. *Nature Communications*, 2024, **15**: 8719-8733

[31] DING R W, QIU S W, GUO X F, *et al*. Space ionizing radiation triggers the formation of peptides and organophosphates on olivine surfaces[J]. *Nature Communications*, 2026, **17**: 3210. DOI:10.1038/s41467-026-69575-x

[32] LIU Y, YING J X, DING K, *et al*. Origin of life experiments onboard Tiangong[J]. *Nature astronomy*, 2024, **8**: 1343

[33] LI Z J, ZHAO L, ZHANG G, *et al*. Optimized combination methods for exploring novel space environment-responsive genes and their roles: Insights from space-flown C. elegans and their implications for astronauts[J]. *International Journal of Radiation Biology*, 2025, **101**: 891-911

[34] ZHANG G, ZHAO L, LI Z J, *et al*. Integrated spaceflight transcriptomic analyses and simulated space experiments reveal key molecular features and functional changes driven by space stressors in space-flown *C. elegans*[J]. *Life Sciences in Space Research*, 2025, **44**: 10-22

[35] ZHANG Y, ZHAO L, SUN Y Q. Using single-sample networks to identify the contrasting patterns of gene interactions and reveal the radiation dose-dependent effects in multiple tissues of spaceflight mice[J]. *npj Microgravity*, 2024, **10**: 45

[36] ZHANG Y, DU X H, ZHAO L, *et al*. Construction of dose prediction model and identification of sensitive genes for space radiation based on single-sample networks under spaceflight conditions[J]. *International Journal of Radiation Biology*, 2024, **100** (5): 777-790

[37] ZHANG Y, ZHAO L, DU X H, *et al*. Integrating single-sample networks and genetic algorithm to estimate radiation dose in multiple tissues of mice under space environment[J]. *Radiation Research*, 2026, **205**(6): 582-596

[38] LIAO H, WANG H P, LIU D N *et al*. Dynamic localization effect of dendritic and eutectic growth patterns stimulated by space fluid flow[J]. *Advanced Materials*, 2025, **37**(47): e08092

[39] WANG H P, LIAO H, WANG Y B, *et al*. Solidification mechanism and microstructure evolution of refractory Nb-Si and Nb-Si-Zr alloys aboard China Space Station[J]. *SCIENTIA SINICA Technologica*, 2025, **55**: 1989-2005

[40] WANG H P, LI H Z, ZHENG C H, *et al*. Eutectic growth kinetics and microscopic mechanical property of refractory Zr57V43 alloy under space and ground conditions[J]. *Acta Materialia*, 2025, **295**: 11

[41] YU J D, ZHANG W, YANG S, *et al*. Recent advances and future prospects of space materials science[J]. *Review of Materials Research*, 2025, **1**(2): 100065

[42] ZHANG P, ZHANG Y, WANG Z L, *et al*. 1D and 3D co-simulation and self-adaptive position control of electrostatic levitation in China's Space Station [J]. *NPJ Microgravity*, 2022, **8**: 29. DOI:10.1038/s41526-022-00215-6

[43] WANG Z H, JIN M, SONG K P, *et al*. Expanded InSe crystal structure with reduced intrinsic defects for high-performance field-effect transistors[J]. *Advanced Materials*, 2025, **38**(4): e06506

[44] JIN R, SUI F R, YU Y L, *et al*. Microgravity-activated high-performance van der Waals InSe ferroelectric semiconductor[J]. *Nature Communications*, 2026, **17**: 3851

[45] JIANG H R, GAO Y F, CAO L, *et al*. Viscosity of a metallic glass-forming liquid by high-rate calorimetry and containerless electrostatic levitation in microgravity[J]. *Journal of Materials Science & Technology*, 2026, **273**: 212-222

[46] ZHANG Z G, TANG M H, DONG C H, *et al*. Phase selection and structural evolution in the solidified FeSe0.5Te0.5 superconductor via gradient temperature quenching[J]. *Acta Materialia*, 2026, **309**: 122071

[47] BAI Y Y, LYU H Y, WANG K, *et al*. The space environment effects and performance evolution of perfluoropolyether-based supramolecular gel lubricants[J]. *SCIENTIA SINICA Technologica*, 2025, **55**(12): 2014-2030 (in Chinese)

[48] WANG L C, ZHANG L Q, ZHENG R H, *et al*. Macroscale superlubrication achieved with shear-thinning semisolid lubricants[J]. *Advanced Materials*, 2024, 2412257. DOI:10.1002/adma.202412257

[49] ZHOU H W, ZOU S Y, OUYANG W Z, *et al*. Long-lived metastable bcc phase in the crystallization of charged colloids under microgravity[J]. *Journal of Colloid and Interface Science*, 2025, **695**: 137841

[50] ZHANG L G, XU B, SHI J, *et al*. Experimental study on condensation heat transfer of FC-72 in a narrow rectangular channel with ellipse-shape pin fins: ground and microgravity experiments[J]. *International Journal of Heat and Mass Transfer*, 2019, **141**: 1272-1287

[51] XU B, CHEN Z Q. Condensation on composite V-shaped surface with different gravity in nanoscale[J]. *Microgravity Science and Technology*, 2019, **31**(5): 603-613

[52] GUO S, LIU M Q, XU B, *et al*. Vapor condensation and droplet directional migration on the surface of asymmetric triangular micropillar array structures using a hybrid thermal lattice Boltzmann method[J]. *International Communications in Heat and Mass Transfer*, 2025, **169**: 109557

[53] WANG J, WU D, ZHAO Y F, *et al*. Spatiotemporal correlation

and chaotic dynamics analysis of annular flow with small volume ratio under microgravity[J]. *Physics of Fluids*, 2026, **38**: 014114.

[54] WU D, TANG W Z, WANG J, *et al*. On Chinese space station: pioneering space experiments unraveling the hydrodynamic instability of annular thermocapillary convection[J]. *Scientific Reports*, 2025, **15**: 24807

[55] HOU M Y, CHENG X H, YANG S, *et al*. Gravity-dependent rate sensitivity in granular intrusion: microgravity experiments and simulations[J]. *NPJ Microgravity*, 2026, **12**: 19

[56] YANG S, CHENG X H, HOU M Y, *et al*. Assessment of the equivalent low-gravity of the granular collapse equipment in the VGR of the Chinese Space Station[J]. *Microgravity Science and Technology*, 2025, **37**: 59

[57] CHENG K, HOU M Y, SUN W, *et al*. Unraveling the role of gravity in shaping intruder dynamics within vibrated granular media[J]. *Communications Physics*, 2024, **7**: 425

[58] WANG W J, JIN K R, ZHENG Z H, *et al*. Research progress on soot formation from C1-C4 hydrocarbon fuel Combustion under microgravity[J]. *Journal of Tsinghua University* (*Science and Technology*), 2025, **65**(09): 1763-1773 (in Chinese)

[59] WANG W J, JIN K R, SHI H Q, *et al*. Variable gravity combustion: new frontiers in flame studies [J]. *NPJ Space Exploration*, 2025, **1**: 14. DOI:10.1038/s44453-025-00016-7

[60] ZHU F, LI D, WANG S F, *et al*. Shape and sooting characteristics of methane laminar-jet diffusion flames in microgravity[J]. *Chinese Journal of Space Science*, 2026, **46**(1): 121-130

[61] LIU K, ZHU F, WANG S F, *et al*. Influence of hydrodynamics on soot process in laminar jet diffusion flame[J]. *Microgravity Science and Technology*, 2025, **37**: 42

[62] LIU Y S, LI X X, WEN Y Z. *et al*. Gas jet flame science experiments aboard the China Space Station[J] *Journal of Tsinghua University* (*Science and Technology*), 2025, **65**(9): 1609-1620 (in Chinese)

[63] CHEN T, YU S, LIU Y C. Effects of pressure on propagation characteristics of methane-air edge flames within two-dimensional mixing layers: A numerical study[J]. *Fuel*, 2021, **301**: 120857

[64] WEN Y Z, LI L F, LI X X, *et al*. Extinction of microgravity partially premixed flame aboard the Chinese Space Station[J]. *Proceedings of the Combustion Institute*, 2024, **40**: 105574. DOI: 10.1016/j.proci.2024.105574

[65] ZHANG D F, LI J T, WANG W Z, *et al*. Compact and robust design of the optical system for cold atom interferometer in space[J]. *Optics Express*, 2025, **33**(17): 35419-35436

[66] LI J T, CHEN X, ZHANG D F, *et al*. Realization of a cold atom gyroscope in space[J]. *National Science Review*, 2025, **12**: nwaf012

[67] ZHAO G D, XIA J, LIU Y, *et al*. Laser cooling alkaline-earth atoms for optical clock in Chinese Space Station[J]. *Chinese Physics Letters*, 2025, **42**(6): 063701

[68] XIA J, WANG W H, ZHAO G Z, *et al*. Optical system for a strontium optical lattice clock aboard the Chinese Space Station[J]. *Review of Scientific Instrument*, 2025, **96**(9): 093201.

[69] SHAO C Y, YU C L, HU L L. Radiation-resistant active fibers for space applications[J]. *Chinese Journal of Lasers*, 2020, **47**(5): 0500014

[70] ZHENG Y, SUN S H, WANG X F, *et al*. Influence of γ-radiation on the output properties of narrow linewidth fiber laser and photo bleaching effect[J]. *High Power Laser and Particle Beams*, 2024, **36**(12): 8-14

[71] GONG Y L, ZHANG J G, LI W B. Application of optical fiber sensing in health monitoring of aerospace composite structure[J]. *Spacecraft Engineering*, 2022, **31**(5): 60-66

Author Biography



GU Yidong An expert in space science and utilization technology and an academician of the Chinese Academy of Sciences (CAS). He currently serves as the Chief Scientist for Space Science of the China Manned Space Engineering Program (CMS). He graduated from the Department of Engineering Physics, Tsinghua University in 1970. His previous posts include Deputy Director of the Cosmic Ray Research Laboratory at the Institute of High Energy Physics (CAS), Director of the National Space Science Center (CAS) and Academy of Opto-Electronics (CAS), Chief Designer and General Commander of the Space Utilization System in CMS, and President of the Chinese Society for Space Research. He led the development of an integrated space-ground utilization technology system for CMS, organized groundbreaking scientific and utilization missions aboard the Shenzhou series spaceship and the Tiangong space laboratory. He also led the planning and demonstration of space science and utilization missions for the China Space Station.
E-mail: ydgu@aoe.ac.cn



ZHANG Wei (Corresponding author) A researcher and director of the Utilization Development Center, Technology and Engineering Center for Space Utilization (CSU) of the CAS. He obtained his Ph.D. in flight vehicle design from the Beijing Institute of Technology (BIT) and joined the Information and Electronics School of the BIT in 2003. After 2012, he joined the CSU and engaged in the strategy planning and mission design for the China Space Station (CSS). He successfully organized a significant number of eminent scientists in the formulation of the scientific mission planning and proposed a systematic and structured scientific research and utilization mission encompassing four major areas for the CSS. Furthermore, he also led the solicitation, evaluation and selection of multiple batches of scientific and utilization projects for the CSS.
E-mail: zhangwei@csu.ac.cn